June 2017

Analysis of a Potential A(H7N9) Influenza Pandemic Outbreak in the U.S.

Walter A. Silva Sotillo
University of South Florida, silvasotillo@mail.usf.edu

Analysis of a Potential A(H7N9) Influenza Pandemic Outbreak in the U.S.

by

Walter A. Silva-Sotillo

A dissertation submitted in partial fulfillment
of the requirements for the degree of
Doctor of Philosophy
Department of Industrial and Management Systems Engineering
College of Engineering
University of South Florida

Major Professor: Tapas K. Das, Ph.D.
Alex Savachkin, Ph.D.
Mingyang Li, Ph.D.
Yicheng Tu, Ph.D.
Ricardo Izurieta, M.D.

Date of Approval:
June 14, 2017

Keywords: Agent Based Simulation, Non-pharmaceutical Intervention, Community Resilience, Time of Infection

Dedication

To my wife, my love and partner in this adventure without whom it would be impossible to achieve. This achievement is also yours. To my two sons who injected emotion and motivation to my life and who are the main reason to me to improve each day.

To my parents, who taught me the importance of study and who made several efforts to give me a profession.

Acknowledgements

I want to acknowledge my advisor, Dr. Tapas K. Das, for his continuous support, trust, guidance, patience and friendship; without him all this journey would be impossible. I am deeply grateful to him for the time invested in conversations, meetings, writings, reviews and advices. I also want to recognize Dr. Alex Savachkin for his support and friendship and Dr. Ricardo Izurieta for sharing his knowledge of expertise to improve my understanding level of epidemiology.

I also want to thanks to all my friends from the PhD program, to those who are still there and still have some years to come and to those who already graduated and shared with me part of their lives.

Table of Contents

Abstract

This dissertation presents a collection of manuscripts that describe development of models and model implementation to analyze impact of potential A(H7N9) pandemic influenza outbreak in the U.S. Though this virus is still only animal-to-human transmittable, it has potential to become human-to-human transmittable and trigger a pandemic. This work is motivated by the negative impact on human lives that this virus has already caused in China, and is intended to support public health officials in preparing to protect U.S. population from a potential outbreak of pandemic scale.

An agent-based (AB) simulation model is used to replicate the social dynamics of the contacts between the infected and the susceptible individuals. The model updates at the end of each day the status of all individuals by estimating the infection probabilities. This considers the contact process and the contagiousness of the infected individuals given by the disease natural history of the virus.

The model is implemented on sample outbreak scenarios in selected regions in the U.S. The sampling results are used to estimate disease burden for the whole U.S. The results are also used to examine the impact of various virus strengths as well as the efficacy of different intervention strategies in mitigating a pandemic burden.

This dissertation, also characterizes the infection time during a A(H7N9) influenza pandemic. Continuous distributions including exponential, Weibull, and lognormal are considered as possible candidates to model the infection time. Based on the negative likelihood, lognormal

distribution provides the best fit. Such characterization is important, as many critical questions about the pandemic impact can be answered from using the distribution.

Finally, the dissertation focuses on assessing community preparedness to deal with pandemic outbreaks using resilience as a measure. Resilience considers the ability to recover quickly from a pandemic outbreak and is defined as a function of the percentage of healthy population at any time.

The analysis, estimations, and metrics presented in this dissertation are new contributions to the literature and they offer helpful perspectives for the public health decision makers in preparing for a potential threat of A(H7N9) pandemic.

Chapter 1: Introduction

1.1 Background

A(H7N9) is a subtype of influenza A viruses that is found in birds including poultry. Since March of 2013, A(H7N9) has been found in several regions of China infecting humans, especially those who are in close contact with poultry either at farms or at markets dealing with poultry. So far, there has been four waves of infections in spring of 2013 and winters of 2013-14, 2014-15, and 2015-16. The fifth wave of infections is currently in progress. As of April 2017, a total of 1393 laboratory-confirmed cases of A(H7N9) infections resulting in 534 deaths [1] have been recorded in several different regions of China spreading at least ten provinces and two municipalities. Additional cases are expected to have occurred in other regions, though have not yet been reported. It may be noted that the outbreaks have occurred in relatively densely populated regions of China that have over 54% of the country's population. The average age of those infected in the first three waves is around 58 [2], and the majority of the infected had a high level of exposure to poultry (e.g., in live bird markets, and some commercial and backyard farms). The higher average age of the infected has not been attributed to the epidemiological features of A(H7N9). This virus is not considered to have acquired the ability to transmit among humans.

From a public health preparedness standpoint, it is essential to assess the possible impact of a pandemic caused by the A(H7N9) virus, potential for which is considered to be high. Similar concerns for an impending pandemic were expressed by the public health community with another potent mutation of influenza virus H5N1 during years 2003-2009. Sporadic outbreaks of H5N1

during there years infected a total of 468 people in 15 countries causing 282 deaths [3]. This virus is also only animal-to-human transmittable. Till date, H5N1 has not acquired the ability to spread human-to-human infection and is still under surveillance.

Researchers have closely examined the A(H7N9) infection scenarios in recent years and published their findings in several papers [4–10]. The findings include estimates of some of the epidemiological parameters. It is important to note that only symptomatic cases of A(H7N9) infections visited the doctor and were documented in the above official reports. It is difficult to assess the percentage of asymptomatic cases, but some researchers have estimated this value to be 50% [11].

An important observation made so far about A(H7N9) is that, though it is highly pathogenic both in humans and birds, infected poultry remains asymptomatic. This makes it difficult to identify the spread of A(H7N9) among poultry. In recent years, the Chinese government has applied containment measures to limit the spread of A(H7N9) virus including culling birds in large numbers and closing live poultry-markets and trading areas [12].

In our effort to assess impact of a pandemic from A(H7N9) virus, we used an updated version of our previously developed AB simulation model [13–15]. The simulation model replicates the dynamics of a given population during a pandemic outbreak by incorporating the demographic information (households, schools, workplaces, and communities), human behavior (including contacts, compliance to quarantine and other public health measures, and travel), epidemiological parameters of the virus (force of infection, incubation and latent periods, basic reproduction number, and fatality rate), and non-pharmaceutical intervention strategies for containment and mitigation. The AB model considers detailed information about the households

and their member compositions (age, sex, work, parental status), distance between individuals, their daily schedules, contact processes, infection process, and disease natural history.

We assumed that during outbreaks, non-pharmaceutical intervention (NPI) strategies are used to contain virus spread. A NPI strategy comprises measures like isolation, quarantine, and school and workplace closures. Parameters defining these measures were chosen in our study based on recommendations found in [15]. Some of our AB simulation model features were adapted from the models presented in [11] and [15].

1.2 Goals and Objectives

The goal of this dissertation is to analyze the impact of a potential influenza pandemic outbreak caused by A(H7N9) virus in the U.S. This goal has been addressed through the following objectives.

1. Improve an existing AB simulation model by incorporating a more detailed approach to estimate the probability of infection.
2. Develop disease burden estimates from a potential A(H7N9) pandemic outbreak affecting the whole United States.
3. Determine the probability distribution characterizing the infection time of a A(H7N9) pandemic outbreak.
4. Assess community preparedness to face pandemic outbreaks using resilience measures.

Objective 1 was achieved by incorporating in an existing simulation model a detailed approach from the literature [11] to estimate the force of infection, a key input to evaluate the probability of infection of a susceptible individual. This updated version of the model was first validated using information from a simulated outbreak in Thailand presented in [11]. Objectives 1

and 2 are considered in the manuscript discussed in Chapter 2. Objective 3 was achieved by analyzing typical continuous distributions using the negative log likelihood as a decision criteria (see Chapter 3). Objective 4 was addressed by developing resilience measures and evaluating the measures for different virus strengths and intervention strategies. Details of these measures are presented in Chapter 4.

1.3 Summary of Manuscripts

The first manuscript estimates the disease burden of a potential A(H7N9) influenza pandemic in the U.S. using an agent-based (AB) simulation model. This AB model has an inherent capacity limitation of simulating only up to five million people. This limitation is attributed to the limited memory availability in standard desktop computers and to the nature of memory usage by the AB model. To work within this limitation, we used a procedure that divides the U.S. in clusters using the number and the density of urban population as predictors. Within each cluster, a subset of states were selected to simulate independent pandemic outbreaks. If a selected state had an urban population below five million, the model considered all urban regions for the simulated outbreak; else, only selected contiguous counties within the state with up to five million people were considered as the outbreak region. The results from the sample states were integrated using a sampling approach, and burden estimates were calculated for each cluster. Results for the clusters were used to obtain estimates for the whole U.S. Infection attack rates (IARs) for transmission scenarios with R_0=1.5 and 1.8 (with 95% C.I.) were found to be 18.78% (17.3-20.27) and 25.05% (23.11-26.99), respectively.

The second manuscript examines the probability distribution that characterizes the infection time for a potential A(H7N9) influenza pandemic outbreak. The data needed for this was

obtained by implementing an AB simulation model on three different scenarios of transmissibility of the A(H7N9) virus. Common continuous probability distributions were analyzed and it was concluded, based on the negative log-likelihood, that the lognormal distribution provides a good fit.

The third manuscript first presents a resilience measure that can de used to assess community preparedness. It then considers an A(H7N9) influenza pandemic outbreak and evaluates the community resilience measures for three different transmissibility scenarios with and without NPIs.

Chapter 2: Estimating Disease Burden of a Potential A(H7N9) Pandemic Influenza Outbreak in the United States

The complete article *Estimating Disease Burden of a Potential A(H7N9) Pandemic Influenza Outbreak in the United States* (submitted to BMC Public Health) can be found in Appendix B.

2.1 Abstract

Since spring 2013, periodic emergence of avian influenza A(H7N9) virus in China has heightened concerns for a possible pandemic outbreak though it is believed that the virus is not yet human-to-human transmittable. Till June 2016, A(H7N9) has resulted in 781 laboratory-confirmed cases of human infections causing 313 deaths (40% fatality rate). This paper presents disease burden estimates from a potential A(H7N9) pandemic outbreak throughout the United States. Estimation method uses a machine learning technique to divide 50 states into three clusters based on urban population size and density, and thereafter employs an agent based (AB) model to simulate outbreaks in selected states from each cluster. Infection attack rates (IARs) stratified by age-groups from these states are used to arrive at disease burden estimate for the whole U.S. For transmission scenarios with R0=1.5 and 1.8, overall IARs (95% C.I.) are found to be 18.78% (17.3-20.27) and 25.05% (23.11-26.99), respectively.

Chapter 3: Analysis of the Infection Time during a Potential H7N9 Influenza Pandemic Outbreak

The complete article *Analysis of the Infection Time from a Potential H7N9 Influenza Pandemic Outbreak* can be found in Appendix C.

3.1 Abstract

Avian influenza viruses have been affecting human populations for a long time since the outbreak in the year 1580, the first recorded in history. Since then, other mutations and reassortments of the influenza viruses (e.g., H1N1, H3N2) have emerged causing pandemics. Recent emergence of A(H7N9) influenza virus in China resulted in 1307 laboratory-confirmed cases of human infections causing 489 deaths (37.4% fatality rate). Researchers have developed early estimates of some of the epidemiological parameters to characterize A(H7N9) virus in China. In this research we examine the distribution that characterizes the infection time from a potential A(H7N9) influenza pandemic outbreak using results from an agent-based (AB) simulation model. The AB model replicates the dynamics of contacts between susceptibles an infected individuals. We examined some of the common continuous probability distributions and conclude, based on the negative log-likelihood, that the lognormal distribution provides a good fit to characterize the infection time.

Chapter 4: Resilience as a Measure of Preparedness for Pandemic Influenza Outbreaks

The complete article *Resilience as a Measure of Preparedness for Pandemic Influenza Outbreaks* can be found in Appendix D.

4.1 Abstract

Periodic emergence of avian influenza A(H7N9) virus in China in recent years has heightened concerns for a possible pandemic outbreak. From a public health preparedness standpoint, it is essential to assess the possible impact of an influenza pandemic and also the resilience of the affected communities, which is the ability to recover quickly from a pandemic outbreak. The aim of this study is to develop community resilience measures and demonstrate their estimation using a simulated pandemic outbreak in a region in the U.S. with a population of 1.2 million. Three scenarios are analyzed with different combinations of virus transmissibility rates and non-pharmaceutical interventions. The agent-based simulation model replicates human interactions, spread of infection and resulting impact on human lives and society. Average percentage of healthy population at any point in time during a pandemic is used to quantify a resilience metric. Based on this new metric, it is demonstrated that resilience is improved between 1.82 and 7.25 times when recommended NPIs are deployed.

Chapter 5: Conclusions

This dissertation is a collection of manuscripts that analyzes different aspects of a relatively new mutation of influenza virus A(H7N9). The key aspect that is studied is the estimation of disease burden from a pandemic outbreak across the whole U.S. from A(H7N9) virus. The other aspects examined are: 1) characterization of infection time during a pandemic, and 2) development of a community resilience measure and examining its use in assessing preparedness in dealing with an influenza pandemic. Detailed conclusions from all three of the studies are presented at the end of each of the manuscripts, and hence will not be repeated here. In the rest of this section, we discuss some of the limitations as well as future extensions of the work presented in the dissertation.

The version of the AB model that was used in this dissertation has limited capability in terms of the total number of people that it can simulate. Due to this limitation, we had to use a clustering and sampling approach to estimate disease burden for the whole U.S. Also, due to the capability limitation, we focused our attention to only urban areas and extrapolated the results to over all areas. This is a simplification, as it is well known that the population dynamics and resulting contact processes in rural areas are different from urban areas. As an extension to this dissertation, a graphical processing unit (GPU) based AB simulation model is being developed. This model is capable of simulating much wider outbreaks with higher number of people (> 100 millions). The model also is much more granular as it incorporates added features like: specific

coordinates for households, businesses, and community places; local and long distances travels; use of antivirals and vaccines; and existing immunity.

We estimated the best probability distribution that describes the infection from among a set of continuous distributions. When NPIs are deployed, infected time exhibits multi-modal behavior which cannot be captured by a classical continuous distribution. However, though our chosen distribution with estimated parameters has acceptable goodness of fit, it can be further improved through perhaps a mixture of distributions. It may also be prudent to classify the infection time data based on age groups. As different influenza viruses tend to have different age-targets.

Resilience metrics estimated in this study were found to be useful in quantifying the efficacies of NPI policies. This helps the decision makers to consider not only the estimate of disease burden but also the resilience of the community. However, future studies in this field may develop new metrics considering cost and other impact measures like loss of productivity.

References

[1] World Health Organization. 2017. Influenza at the human-animal interface Summary and assessment, 16 March to 20 April 2017. Available at http://www.who.int/influenza/ human_animal_interface/ Influenza_Summary_IRA_HA_ interface_04_20_2017.pdf?ua=1. Released on April 2017. Accessed on May 19, 2017

[2] World Health Organization. 2017. P. Wu, Z. Peng, V. J. Fang, L. Feng, T. K. Tsang, H. Jiang, and et al., "Human infection with influenza a (h7n9) virus during 3 major epidemic waves, china, 2013–2015," Emerging infectious diseases, vol. 22, no. 6, p. 964, 2016.

[3] World Health Organization, "Cumulative number of confirmed human cases for avian influenza a(h5n1) reported to who, 2003-2016," 2016. Available: fhttp://www.who.int/influenza/human animal interface/EN GIP20160509cumulativenumber H5N1cases.pdf?ua=1g. Online; accessed 1-June-2016

[4] Z. Liu and C.-T. Fang, "A modeling study of human infections with avian influenza a h7n9 virus in mainland china," International Journal of Infectious Diseases, vol. 41, pp. 73–78, 2015.

[5] X. Zhou, Y. Li, Y. Wang, J. Edwards, F. Guo, A. C. Clements, and al., "The role of live poultry movement and live bird market biosecurity in the epidemiology of influenza a (h7n9): DISEASE BURDEN FOR POTENTIAL A(H7N9) IN THE U.S. 11 A cross-sectional observational study in four eastern china provinces," Journal of Infection, vol. 71, no. 4, pp. 470–479, 2015.

[6] M. Husain, "Avian influenza a (h7n9) virus infection in humans: Epidemiology, evolution, and pathogenesis," Infection, Genetics and Evolution, vol. 28, pp. 304–312, 2014.

[7] V. K. Nguyen and E. A. Hernandez-Vargas, "Identifiability challenges in mathematical models of viral infectious diseases," IFACPapersOnLine, vol. 48, no. 28, pp. 257–262, 2015.

[8] T. Wang, "Dynamics of an epidemic model with spatial diffusion," Physica A: Statistical Mechanics and its Applications, vol. 409, pp. 119–129, 2014.

[9] J. Li, G.-Q. Sun, and Z. Jin, "Pattern formation of an epidemic model with time delay," Physica A: Statistical Mechanics and its Applications, vol. 403, pp. 100–109, 2014.

[10] L. N. Murillo, M. S. Murillo, and A. S. Perelson, “Towards multiscale modeling of influenza infection,” Journal of theoretical biology, vol. 332, pp. 267–290, 2013.

[11] N. M. Ferguson, D. A. Cummings, S. Cauchemez, C. Fraser, S. Riley, M. Aronrag, and et al., “Strategies for containing an emerging influenza pandemic in southeast asia,” Nature, vol. 437, no. 7056, pp. 209–214, 2005.

[12] Cable News Network, “Chinese authorities kill 20,000 birds as avian flu toll rises to 6,” 2013. Available:fhttp://www.cnn.com/2013/04/05/world/asia/china-bird-flu/index.htmlg. Accessed on June 1st, 2016

[13] T. K. Das, A. A. Savachkin, and Y. Zhu, “A large-scale simulation model of pandemic influenza outbreaks for development of dynamic mitigation strategies,” Iie Transactions, vol. 40, no. 9, pp. 893–905, 2008.

[14] A. Uribe-S´anchez, A. Savachkin, A. Santana, D. Prieto-Santa, and T. K. Das, “A predictive decision-aid methodology for dynamic mitigation of influenza pandemics,” OR spectrum, vol. 33, no. 3, pp. 751–786, 2011.

[15] D. L. Martinez and T. K. Das, “Design of non-pharmaceutical intervention strategies for pandemic influenza outbreaks,” BMC public health, vol. 14, no. 1, p. 1, 2014.

Appendices

Appendix A: Estimating Disease Burden of a Potential A(H7N9) Pandemic Influenza Outbreak in the United States

Estimating Disease Burden of a Potential A(H7N9) Pandemic Influenza Outbreak in the United States

Walter Silva, Tapas K. Das and Ricardo Izurieta

Walter A. Silva is with the Department of Industrial and Management System Engineering, University of South Florida, Tampa, FL, 33620. USA.

Tapas K. Das is with the Department of Industrial and Management System Engineering, University of South Florida, Tampa, FL, 33620. USA.

Ricardo Izurieta is with the College of Public Health, University of South Florida, Tampa, FL, 33620. USA.

Keywords: Influenza, Influenza A Virus -H7N9 Subtype, Agent-based simulation model, Cluster Analysis, Sampling Studies.

Contact Information:

Walter A. Silva – corresponding author
e-mail: silvasotillo@mail.usf.edu.
Telephone: +1-(813)-324-0178

Tapas K. Das
e-mail: das@usf.edu
Telephone: +1-(813)-843-0285

Ricardo Izurieta
e-mail: rizuriet@health.usf.edu
Telephone: +1-(813)-974-8913

ABSTRACT

Aim

Since spring 2013, periodic emergence of avian influenza A(H7N9) virus in China has heightened the concern for a possible pandemic outbreak, though it is believed that the virus is not yet human-to-human transmittable. Till January 2017, A(H7N9) has resulted in 918 laboratory-confirmed cases of human infections causing 359 deaths. The aim of this paper is to present disease burden estimates from a potential A(H7N9) pandemic outbreak spread over all 50 contiguous states of the U.S. with a total population of 307 million.

Method

The method uses a machine learning technique to divide 50 states in the U.S. into a small number of clusters based on urban population size and density. Thereafter, for a few selected states in each cluster, the method employs an agent-based (AB) model to simulate influenza pandemic outbreaks. The model uses demographic data published by U.S. Census bureau, and epidemiological data from published research reports on H7N9. A few selected non-pharmaceutical interventions (NPIs) were applied on the outbreaks. For two different epidemiological scenarios with $R_0 = 1.5$ and 1.8, infection attack rates (IAR) and the number of deaths were estimated.

Results

Overall IARs (95% C.I.) for $R_0 = 1.5$ and 1.8 were found to be 18.78% (17.3 – 20.27) and 25.05% (23.11 – 26.99), respectively. The corresponding number of deaths (95% C.I.), in millions, were estimated to be 23.9 (22.0 – 25.8) and 31.9 (29.4 – 34.6).

Conclusions

Our results represent a worst-case scenario where no antivirals or vaccines are administered and the pandemic is considered to have spread over the whole contiguous territory of the U.S. The results are also likely to be somewhat higher due to the fact that only dense urban regions (around 3% of the geographic area) with approximately 81% of the population were used for simulating sample outbreaks. Outcomes from these simulations were extrapolated over the remaining 19% of the population spread sparsely over 97% of the area. Furthermore, the full extent of possible NPIs, if deployed, could also have lowered the estimates.

I. INTRODUCTION

A(H7N9) has infected humans in China in three waves, spring 2013, winter 2013-14, and winter 2014-15. The fourth wave is currently in progress. As of January 2017, a total of 918 laboratory-confirmed cases of A(H7N9) infections have been recorded in China causing 359 deaths [1]. Figure 1 depicts the outbreak locations which are in relatively densely populated regions with over 54% of China's population. The reported average ages of those infected in the first three waves are 61, 57, and 56, respectively [2]. However, the relative high age of those infected has not been

attributed as an epidemiological characteristic of A(H7N9). Instead, it is conjectured to be a function of the higher level of exposure to poultry for elderly. Though most of the infections are known to be isolated cases, exceptions were noted where human-to-human transmission may have occurred. For example, there were at least sixteen clusters of three infected family members and one cluster of two infected family members [3]. However, there is still lack of sustained evidence of human-to-human transmission [1].

Wave ⟶	1st	2nd	3rd	4th (ongoing)
	spr '13	wint-spr '13-'14	wint-spr '14-'15	wint-spr '15-'16
# Infected	133	320	226	102
# Dead	48	127	100	38

#	Province / Municipality	% of Total Population
1	Beijing	1.46
2	Shandong	7.15
3	Henan	7.02
4	Anhui	4.44
5	Jiangsu	5.80
6	Shanghai	1.72
7	Hubei	4.27
8	Jiangxi	3.33
9	Hunan	4.90
10	Zhejiang	4.06
11	Guangdong	7.79
12	Fujian	2.75

Fig. 1. Extent and impact of waves of A(H7N9) outbreaks in China

Experts fear that A(H7N9) could become human-to-human transmittable and cause a pandemic. Hence, from a public health preparedness standpoint, it is essential to assess the possible impact (disease burden) of a A(H7N9) pandemic. A significant fear of a H5N1 pandemic outbreak existed during the years 2003-2009, when the virus infected a total of 468 people with 282 deaths in 15 countries [4]. These numbers were updated in 2015 to 844 infected and 449 deaths [5]. Research papers published in 2005 [6] and 2006 [7] critically examined the impact of potential H5N1 outbreaks. The disease burden in the U.S. from the H1N1/09 outbreak has been estimated to be 60.8 million infections and 12,469 deaths [8].

Examinations of A(H7N9) infections [9–15] present some of the epidemiological parameters for the virus. A comparison of A(H7N9) parameters, with those for H5N1 is shown in Table I [16]. A(H7N9) is highly pathogenic both in humans and birds but infected poultry remain asymptomatic and do not die.

The objective of this paper is to present an estimate of the disease burden of a potential A(H7N9) influenza pandemic in the U.S. The estimate is obtained using our agent-based simulation model which were published in previous versions [17–20]. A systematic review of the pandemic simulation models can be found in [21]. We implemented the AB model separately in a few selected states representing the U.S. and used their results to estimate burden on U.S. The AB model is limited to simulating up to five million people per run. This is due to limited memory capacity in desktop computers and how memory is utilized by the AB model. The simulation model replicates the dynamics of pandemic outbreak by incorporating the demographic information (households, schools, workplaces, and communities), human behavior (contacts, compliance to quarantine and other public health measures, and travel), epidemiological parameters of the virus (force of infection, incubation and latent periods, basic reproduction number (R_0), and fatality rate), and non-pharmaceutical interventions. The AB model considers household member compositions (age, sex, work, parental status), distance between individuals and their daily movements, contact processes, infection process, and disease natural history.

TABLE I

COMPARATIVE PARAMETERS FOR H5N1 AND H7N9

Characteristic	H5N1	H7N9
Incubation (days)	3.3 ± 1.5	3.1 ± 1.4
Latent Period (days)	2.15	< 3
Fatality risk	$70\%(China)$	$32\%(China)$
*Admission to death	$5.7\ days$	$12\ days$
*Admission to discharge	$18.7\ days$	$41.7\ days$
*Median Age	26	62
*Poultry exposure	71%	75%

* Presented for information only; not used in our model

In order to select the representative states to simulate A(H7N9) outbreak, we first classified 50 states into clusters using urban population size and density as predictors. These are highly correlated to the spread of influenza virus. The classification technique yielded a number of clustering alternatives (Figure 2), of which we selected the 3-cluster alternative. Clusters 1 to 3 contained states in an increasing order of predictor value combinations. Figure 3 depicts the cluster designation for the states. We selected New Mexico from cluster 1, Colorado and Oregon from cluster 2, and California and New York from cluster 3. Selection of these five states was influenced by a recent paper [22] that presents disease burden estimates for seasonal influenza.

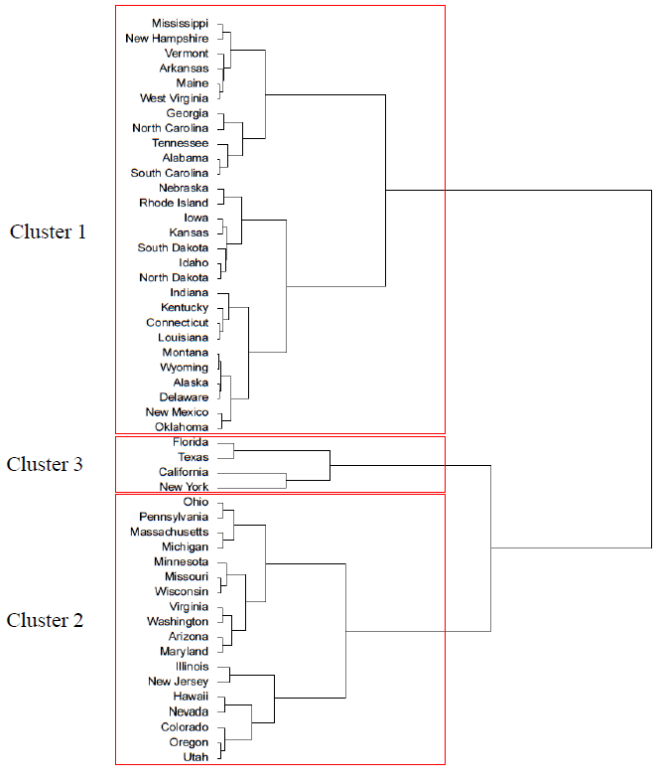

Fig. 2. Dendrogram with the list of states contained within three clusters

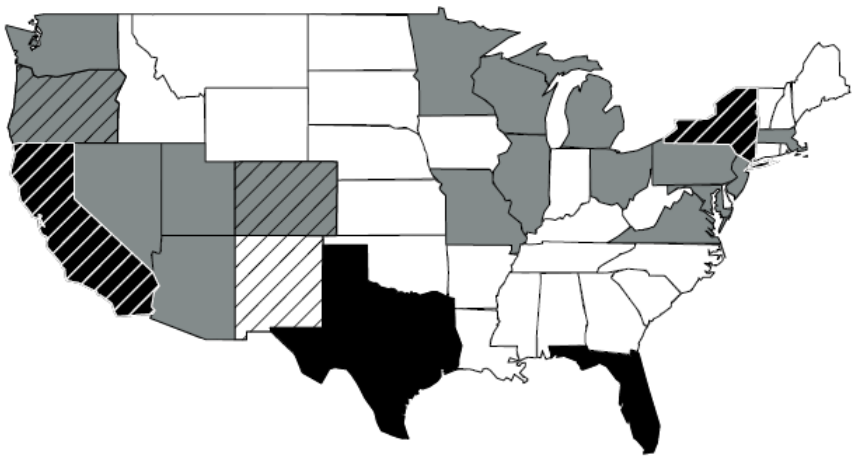

Fig. 3. Map of 48 states of U.S. designated to clusters 1(white), 2(gray), 3(black). States marked with lines were selected for outbreak simulation. Not shown in the figure are Alaska (cluster 1) and Hawaii (cluster 2).

For California and New York with urban population sizes greater than five million, we selected a number of urban counties within each state with a cumulative population less than or equal to five million. While for Colorado, Oregon, and New Mexico we simulated their total urban population, each less than 5 million. Our focus on urban population was guided by the fact that approximately 81% of the population of the selected states reside in dense urban regions constituting on average 3.4% of the land area. We used latest census data to extract information on households, workplaces, and schools. We implemented a non-pharmaceutical intervention (NPI) strategy comprising measures like isolation, quarantine, school and workplace closures. Pharmaceutical interventions (vaccines and antivirals) were not considered.

The remaining paper is organized as follows. In Section 2, we discuss the clustering technique, the AB simulation model and its main features, and the parameter estimation method from stratified data. Section 3 presents validation of our AB model. Section 4 presents model parameter values. Results and conclusions are presented in Section 5 and 6, respectively.

II. METHODS

A. Clustering Method

We used a hierarchical clustering method. Predictor values were first normalized by subtracting from each the corresponding mean and dividing by the corresponding standard deviation. The method begins by assigning each state to a separate cluster (50 clusters at start). Then it calculates the Euclidean distances between the predictor vectors (size, density) of all cluster pairs. Identifies the cluster pair with the smallest distance and combines them into one cluster. This reduces the number of original clusters by one, and for the combined cluster, its predictor vector is assigned as the centroid of the predictor vectors of the two constituent clusters. At the next step, the distances between the clusters are updated, and the process repeats until all clusters are combined into one single cluster. A line diagram (called, dendrogram) is then used in selecting an acceptable number of clusters considering a desired level of similarity within each cluster. We implemented the clustering method by first using *preprocess* function within the *Caret* package of *R* library to normalize the data. Thereafter, we used the *predict*, *dist*, and *hclust* functions within the *stats* package of *R* library for the remaining steps of the method. *R* is a free and open source language and environment for statistical analysis (https://cran.r-project.org/).

B. AB Simulation Model

We updated an existing AB model [17–19] by incorporating the method for estimating force of infection found in [6]. The model mimics the contact process and tracks each individual in an outbreak region using their scheduled hourly movements within the mixing groups: households, places (schools and workplaces), and communities. The model begins by generating the mixing groups and the individuals according to the census and demographic data. Each individual is assigned a household, a place, and a subset of the community locations to visit daily. At the end

of each day, the model estimates the force of infection for each susceptible individual. The force of infection is then used to determine if an individual becomes infected. AB model components are described next.

B1. Disease Natural History

An infected individual simultaneously begins a latency and an incubation period (based on parameters given in Table I). The individual displays symptoms (unless asymptomatic) at the end of the incubation period, and becomes infectious after the latent period is complete. Following the infectiousness period, an infected either recovers or dies. Recovered becomes immune. As no estimate of the proportion of asymptomatic cases is reported for A(H7N9) so far, we assumed it to be 50% as considered in previous studies [6]. The duration of infectiousness for each case is calculated using a lognormal random generator with parameters given in Table VI.

B2. Infection Model

An individual *i* is considered to accumulate force of infection λ_i in his/her home, in places, and in community locations. It is calculated as in [6]:

$$\lambda_i = \sum_{k|h_k=h_i} \frac{I_k \beta_h \kappa(t-\tau_k)\rho_k[1+C_k(\omega-1)]}{n_i^{\alpha}} + \sum_{j,k|l_k^j=l_i^j} \frac{I_k \beta_p^j \kappa(t-\tau_k)\rho_k\left[1+C_k(\omega\psi_p^j(t-\tau_{k)}-1)\right]}{m_i^j} + \frac{\sum_k I_k \varsigma(a_i)\beta_c \kappa(t-\tau_k)\rho_k f(d_{i,k})[1+C_k(\omega-1)]}{\sum_k f(d_{i,k})} \quad (1)$$

The first component in (1) expresses the force experienced by susceptible individual *i* at home from other infected household members *k*. The second component captures the force experienced at places (schools and workplaces) when a susceptible *i* is in the same place as infected *k*. The third component considers all infected members of the community as a function of their distances from the susceptible *i*. The parameters of (1) are defined in Table II. λ_i is calculated at the end of each day for all susceptible *i* and the probability of infection is obtained as $1 - exp^{-\lambda_i}$. It is assumed that if not infected by the end of a day, λ_i is reset to zero.

TABLE II

PARAMETERS RELATED TO THE FORCE OF INFECTION

Parameter	Description
I_k	1 if infected and 0 otherwise
β_h	household transmission parameter
β_p^j	place transmission parameter
β_c	community transmission parameter
$\kappa(t-\tau_k)$	infectiousness at time $(t-\tau_k)$ since infection
$\psi_p^j(t-\tau_k)$	factor by which within-place contact rates change for symptomatic severe infection (reflecting sickness-induced absenteeism)
$f(d_{i,k})$	a function of distance $d_{i,k}$ between individuals i and k
$\zeta(a_i)$	relative travel-related contact rate of an individual of age a_i
ρ_k	relative infectiousness of individual k
C_k	1 if individual k is a severe infection, 0 otherwise
ω	2, infectiousness of a severe infection relative to a mild one
n_i^α	number of people in the household of individual i
α	power that determines the scaling of household transmission rates with household size
m_i^j	number of people in the place type j of individual i

B3. Non-Pharmaceutical Intervention

We considered isolation of symptomatic infected individuals at home for a specific duration with isolation compliance of 53% for adult workers and 57.5% for non-workers [19]. A compliant infected individual is assumed to stay home all day. We consider an isolation threshold of one day (that is, on average an individual diagnosed with infection does not begin isolation until the day after) and isolation duration of seven days, based on the disease natural history.

We also considered household quarantine that restricts the movement of susceptible household members when one or more members are infected. Household quarantine parameters were considered same as for individual isolation. Children were assumed to fully comply with isolation. A partial school closure approach closed a classroom when a threshold of newly infected children in the classroom was reached. A threshold for the number of closed classrooms was used to close a school.

We used a threshold value of one for both the classroom closure and school closure and closure of 21 days. Workplace closure strategy was similar to that of school closure where each

department/group was treated like a classroom. The thresholds were: three cases to close a department, 30% of the departments closed to close a workplace, and seven days for closure duration.

C. Disease Burden (IAR) Calculation from Estimates Stratified by Cluster and Age-Groups

We first calculated the mean and C.I. of the IAR, for all three age-groups (indexed by *a*) in all sampled states (indexed by *i*) within each cluster (indexed by *j*), using replicated results of the AB simulation model. The $100(1-\alpha)\%$ C.I. was calculated as $\hat{p}_{ij}^{a} \pm t_{\alpha/2,n-1}\frac{s}{\sqrt{n}}$, where $\hat{p}_{ij}^{a}$ denotes the mean IAR, n represents the number of simulation replicates, and *s* represents the standard deviation of the replicated estimates. Mean IAR values for the clusters were obtained by combining the values of $\hat{p}_{ij}^{a}$ into $\hat{p}_{j}^{a}$ using the expression below [23].

$$\hat{p}_{j}^{a} = \frac{1}{n_{j}^{a}}\sum_{i=1}^{S_j} n_{ij}^{a}\hat{p}_{ij}^{a}, \tag{2}$$

where S_j denotes the total number of selected states that were simulated within cluster *j*, and n_{ij}^{a} represents the size of the urban population in state *i* within cluster *j* for age-group *a*. Note that $n_{j}^{a} = \sum_{i=1}^{S_j} n_{ij}^{a}$ is the total urban population for the selected states in cluster *j* for age-group *a*. The $100(1-\alpha)\%$ C.I. on the IAR estimate for each age group within a cluster was obtained as $\hat{p}_{j}^{a} \pm t_{\alpha/2,n-1}\frac{s_{j}^{a}}{\sqrt{n}}$. The pooled standard deviation s_{j}^{a} was calculated from the replicated estimates of IAR for each selected state within a cluster as the square root of $\left[(n-1)s_{j1}^{a^2} + \cdots + (n-1)s_{jk}^{a^2}\right]/[k(n-1)]$, where *k* is the number of selected states in cluster *j*, n is the number of simulation replicates, and s_{jk}^{a} is the standard deviation of replicated estimates for age-group *a* in state *k* within cluster *j*. Hereafter, we combined the IAR estimates from all clusters into one value for each age-group using

$$\hat{p}^{a} = \frac{1}{N^{a}}\sum_{j=1}^{C} N_{j}^{a}\hat{p}_{j}^{a}, \tag{3}$$

where C denotes the number of clusters, N_{j}^{a} denotes the total population of all the states in cluster *j* in age-group *a*, and N^{a} denotes the total population in the country in age-group *a*. It may be noted that the estimate $\hat{p}^{a}$ has a variance V^{a} from two sources of variability: 1) due to sampling: a sample population from each cluster is used to estimate $\hat{p}_{j}^{a}$, which is then considered to hold good for the whole cluster population, 2) due to simulation based estimation: $\hat{p}_{j}^{a}$'s are obtained from $\hat{p}_{ij}^{a}$, which are estimated from simulation model with inherent variability. It can be argued that these two sources of variability are independent. We obtained the variance due to sampling V_{1}^{a} as follows [24],

$$V_{1}^{a} = \frac{1}{(N^{a})^2}\sum_{j=1}^{C}\left(N_{j}^{a}\right)^2\left(\frac{N_{j}^{a}-n_{j}^{a}}{N_{j}^{a}}\right)\left(\frac{\hat{p}_{j}^{a}\left(1-\hat{p}_{j}^{a}\right)}{n_{j}^{a}-1}\right). \tag{4}$$

The variance due to simulation V_{2}^{a} was obtained as the pooled variance from the variance estimates (s_{j}^{a}) of the three clusters as $V_{2}^{a} = \left[((n-1)s_{1}^{a^2} + (n-1)s_{2}^{a^2} + (n-1)s_{3}^{a^2}\right]/[3(n-1)]$, where

n is number of simulation replicates per cluster. A $100(1-\alpha)\%$ C.I. was calculated as $\hat{p}^a \pm t_{\alpha/2,n-1}\sqrt{V^a/n}$. Finally, we obtained a single estimate of IAR ($\hat{p}$) for the whole U.S. across all age-groups $a \in \{1,2,\dots,L\}$ using (3) and substituting in the equation N, N^a and $\hat{p}^a$ for N^a, N_j^a and $\hat{p}_j^a$, respectively, and summing over a = 1 through L. The variance V on the overall IAR estimate was obtained by pooling variance values V^a from the three age-groups. A $100(1-\alpha)\%$ C.I. was calculated as $\hat{p} \pm t_{\alpha/2,n-1}\sqrt{V/n}$.

III. MODEL VALIDATION

We validated our model by replicating a H5N1 outbreak study for Southeast Asia [6]. The study considered 85 million people. We considered a subset of people (5M) and proportionately adjusted down the number of households, schools, workplaces, and community locations. As in [6] we considered two different R_0 (1.5 and 1.8) values and ran ten replicates for each. For $R_0 = 1.5$, the average IAR ($\bar{X}$) is 34.58% with a standard deviation (s) of 5.24, and 95% C.I. of [30.83 - 38.33]. The IAR reported in [6] for $R_0 = 1.5$ is 33%, which is within our C.I. Our corresponding values for $R_0 = 1.8$ are 55.7%, 8.16, and [49.86 - 61.54], respectively. The IAR reported in [6] is 50%.

IV. DISEASE BURDEN ESTIMATION: PRELIMINARIES

The AB simulation model was implemented considering only the urbanized regions of the five selected states. Table III shows the population sizes and their distribution between urban and rural regions. Urban population of Colorado, New Mexico, and Oregon are below the 5 million threshold of our AB model capacity. Hence, for these states, the AB model used total urban population as sample sizes. For example, Colorado was simulated using the total urban population of 4.62M as the sample size comprising 1.19M for ages ≤ 19, 2.83M for ages 20 – 64, and 0.59M for ages 65 and above (see Table IV). For California and New York, we adopted a proportional sampling approach. For example, California has 9.7M people for age-group ≤ 19 years and 22.4M and 4.74M for age-groups 20 – 64 years and ≥ 65 years, respectively. The AB model used the family composition features from the U.S. census to randomly generate a total of (9.7/36.8)x5M children, (22.4/36.8)x5M adults up to age 64, and (4.74/36.8)x5M adults 65 and above. Also using census data, the model first creates a proportional number of households in a region and then populates each household following the average proportion of children and adults in various age-groups in U.S. families as presented in Table V. Thereafter, the model generates the places (schools and workplaces) using census data in [24] and [25], and randomly assigns each individual to a place based on the age-group. Beyond households and places, the model also considers movements of the individuals in the community within the state for daily errands. Same proportions given in Table V are used for all five selected states.

TABLE III

URBAN AND RURAL POPULATION DISTRIBUTIONS IN THE STATES SELECTED FOR SIMULATION

Region	Total pop	Urban pop(%)	Urban pop	Urban area(%)	Urban density pop/sq mile
California	$38.80M$	94.95	$36.8M$	5.28	4304
Colorado	$5.36M$	86.15	$4.62M$	1.47	2836
New Mexico	$2.09M$	77.43	$1.62M$	0.68	1929
New York	$19.75M$	87.87	$17.35M$	8.68	4161
Oregon	$3.97M$	81.03	$3.22M$	1.15	2804

TABLE IV

SIZE OF SAMPLED POPULATION AND IAR OUTCOMES FOR AGE-GROUPS IN STATES SELECTED FOR SIMULATION

$<= 19yrs$	Urban population	Sample size	$\hat{p}^a_{ij}$ $(R_0 = 1.5)$	$\hat{p}^a_{ij}$ $(R_0 = 1.8)$
California	$9.7M$	$1.32M$	0.3272	0.4197
Colorado	$1.19M$	$1.19M$	0.2782	0.3797
New Mexico	$0.43M$	$0.43M$	0.2461	0.3299
New York	$4.18M$	$1.21M$	0.3172	0.4176
Oregon	$0.77M$	$0.77M$	0.2572	0.3777
$20 - 64yrs$				
California	$22.4M$	$3.04M$	0.1612	0.2113
Colorado	$2.83M$	$2.83M$	0.1431	0.1906
New Mexico	$0.94M$	$0.94M$	0.1385	0.1856
New York	$10.62M$	$3.06M$	0.1524	0.2007
Oregon	$1.93M$	$1.93M$	0.1419	0.1866
$65 + yrs$				
California	$4.74M$	$0.64M$	0.1607	0.2291
Colorado	$0.59M$	$0.59M$	0.1447	0.1926
New Mexico	$0.25M$	$0.25M$	0.1248	0.1615
New York	$2.55M$	$0.73M$	0.1589	0.2144
Oregon	$0.51M$	$0.51M$	0.1386	0.1872

TABLE V

U.S. HOUSEHOLD COMPOSITION AND AGE DISTRIBUTION PER CENSUS 2014

Household Composition		
# adults	# children	Proportion
1	0	28%
1	1	4%
2	0	31%
1	2	4%
2	1	13%
1	3	1%
2	2	13%
1	4	1%
2	3	6%

Age distribution of households members			
Children		Adults	
Age range	Proportion	Age range	Proportion
$[0-5]$	24%	$[23-29]$	16%
$[6-9]$	23%	$[30-64]$	67%
$[10-14]$	25%	$[65+$	17%
$[15-17]$	13%		
$[18-22]$	15%		

The AB model initiated each outbreak by introducing six infected individuals. The parameter values used to calculate λ_i using (1) are shown on Table VI (for $R_0 = 1.8$). To calculate the third component of λ_i, we assumed, for simplicity, that each day an individual (susceptible or infected) travel within or outside of their county of residence for errand or leisure. Distance $d_{i,k}$ was obtained as the distance (in kilometers) between the center of the county locations for susceptible i and infected k. Similar parameters were also used in [26].

TABLE VI

PARAMETER VALUES USED IN THE AB MODEL FOR $R_0 = 1.8$

Parameter	Description
β_h	$0.47/day$, $(0.39/day, for\ R_0 = 1.5)$
β_p^j	$0.94/day$,$(0.78/day, for\ R_0 = 1.5)$ (for schools) and $0.47/day$,$(0.39/day, for\ R_0 = 1.5)$ (for workplaces)
β_c	$0.075/day$, $(0.06/day, for\ R_0 = 1.5)$
$\kappa(t-\tau_k)$	from lognormal distribution with: $\delta = -0.72$ and $\gamma = 1.8$
$\psi_p^j(t-\tau_k)$	0.2 (for schools) and 0.5 (for workplaces) only when the elapsed time since the onset of infection is greater than the latent period 0.25 days; the value of ψ_p^j is 0 otherwise
$f(d_{i,k})$	$\frac{1}{[1+\frac{d_{i,k}}{a}]^b}$, with $a = 35km$ and $b = 6.5$
$\zeta(a_i)$	$\zeta(a_i) = 100\%$ if age $\in [20-65]$, 75% if age $\in [15-20]$ and $[65-70]$, 50% if age $\in [10-15]$ and $[70-75]$, 25% if age $\in [5-10]$ and $[75-85]$, 0% if age $\in [0-5]$
ρ_k	1
C_k	1 if individual k is a severe infection, 0 otherwise
ω	2
n_i^α	obtained from the households generated by the model
α	0.8
m_i^j	obtained from the population and places generated by the model

The AB simulation model gives us as outcome the mean IAR values ($\hat{p}_{ij}^a$) displayed on Table IV. We used the estimated values of $\hat{p}_{ij}^a$ and n_{ij}^a to estimate $\hat{p}_j^a$, using (2), IAR per age-group within a cluster. These values were then combined to obtain estimate of IAR for each age-group ($\hat{p}^a$) in the whole U.S. Finally, IAR values for all age-groups were combined to obtain the overall IAR estimate ($\hat{p}$).

V. DISEASE BURDEN ESTIMATION: RESULTS

Ten replicates of independent simulation runs were made for each of the five selected states from three density clusters. We collected age-stratified output data (IAR). Figures 4, 5 and 6 show the IARs and their C.I.s, which can be seem to be generally higher for states/clusters with higher population density.

The IARs for the five states were then used to calculate IARs for the corresponding clusters. Tables VII and VIII show IARs and number of infected cases per age-group within each cluster combined. IAR estimates across all clusters within the age-groups ($\hat{p}^a$ in (3)) and across all age-groups ($\hat{p}$), and the number of fatalities are shown in Table IX.

The IAR estimates were compared with IAR estimates for other viruses as shown in Table X. Simulation-based estimates of IAR for both H5N1 and A(H7N9) were found to be much lower

than the field estimate for H1N1/2009. We conjecture that the lower IAR estimates are due to lower estimates of the force of infection, for which the parameters were estimated from only animal-to-human transmittable cases of outbreaks.

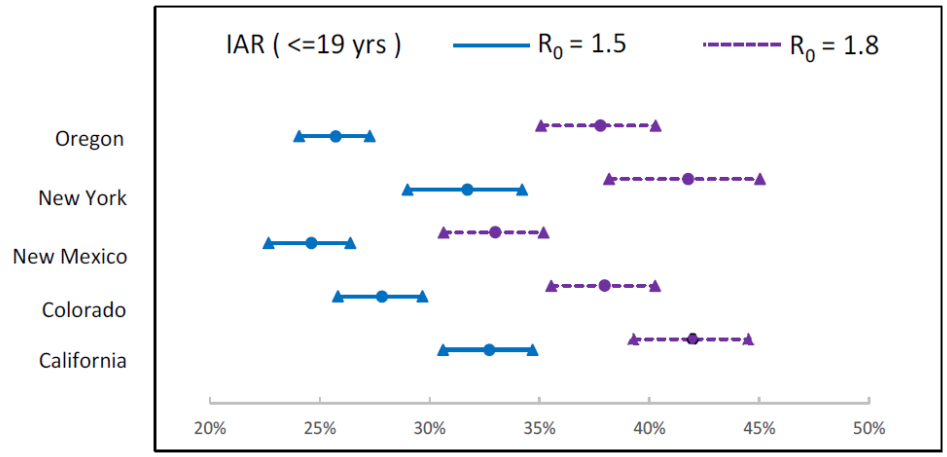

Fig. 4. C.I. for infection attack rates for age-group ≤ 19yrs

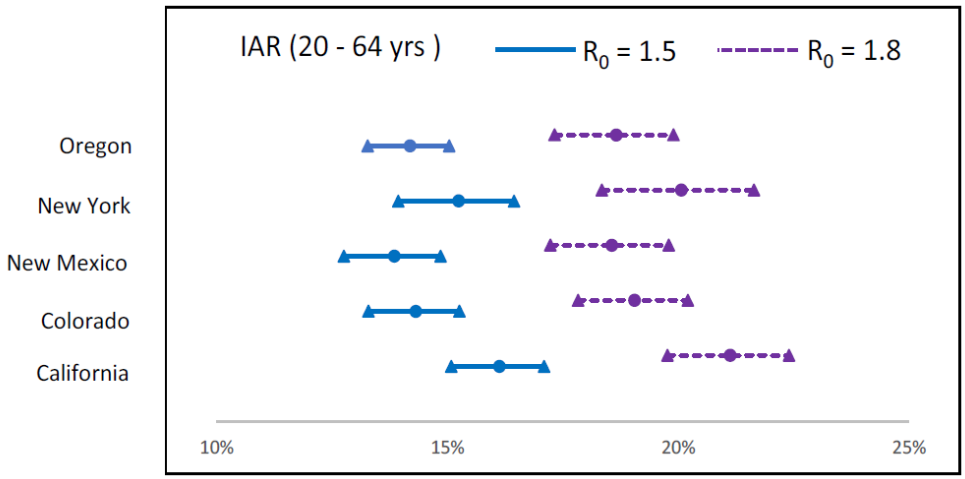

Fig. 5. C.I. for infection attack rates for age-group 20 – 64 yrs

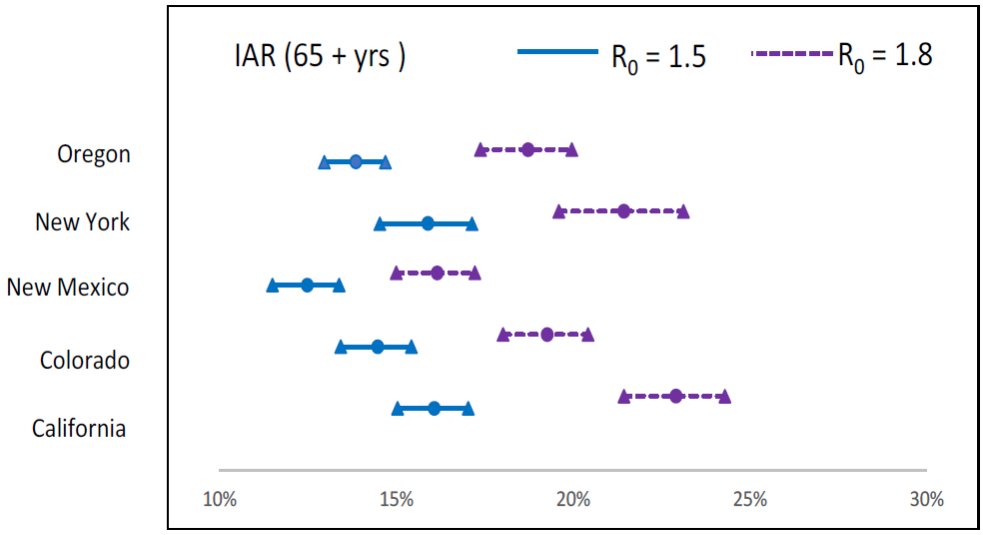

Fig. 6. C.I. for infection attack rates for age-group 65+ yrs

TABLE VII

IAR (%) PER CLUSTER AND AGE-GROUP FOR U.S. WITH 95% C.I.

	IAR (R_0=1.5)			IAR (R_0=1.8)		
	Cluster 1	Cluster 2	Cluster 3	Cluster 1	Cluster 2	Cluster 3
<=19 yrs	24.61	27.00	32.41	32.99	37.89	41.91
	(22.67 - 26.55)	(25.17 - 28.83)	(29.98 - 34.84)	(30.63 - 35.35)	(35.31 - 40.47)	(38.74 - 45.08)
20-64 yrs	13.85	14.26	15.84	18.56	18.89	20.79
	(12.76 - 14.94)	(13.29 - 15.23)	(14.66 - 17.02)	(17.23 - 19.89)	(17.61 - 20.17)	(19.24 - 22.34)
65+ yrs	12.48	14.18	16.01	16.15	19.01	22.39
	(11.5 - 13.46)	(13.21 - 15.15)	(14.8 - 17.22)	(14.99 - 17.31)	(17.72 - 20.3)	(20.72 - 24.06)

TABLE VIII

NUMBER OF INFECTED CASES PER CLUSTER AND AGE-GROUP FOR U.S. WITH 95% C.I.

	Number of infected* (R_0=1.5)			Number of infected* (R_0=1.8)		
	Cluster 1	Cluster 2	Cluster 3	Cluster 1	Cluster 2	Cluster 3
<=19 yrs	5.65	8.55	13.20	7.57	12.01	17.07
	(5.2 - 6.09)	(7.97 - 9.13)	(12.21 - 14.19)	(7.03 - 8.12)	(11.19 - 12.82)	(15.78 - 18.36)
20-64 yrs	7.22	10.64	7.90	9.68	14.10	10.37
	(6.65 - 7.79)	(9.92 - 11.37)	(7.31 - 8.49)	(8.98 - 10.37)	(13.14 - 15.05)	(9.6 - 11.14)
65+ yrs	1.62	2.62	2.37	2.09	3.51	3.31
	(1.49 - 1.74)	(2.44 - 2.79)	(2.19 - 2.55)	(1.94 - 2.24)	(3.27 - 3.74)	(3.06 - 3.56)

* in millions

TABLE IX

IAR (%) AND NUMBER OF INFECTED CASES PER AGE-GROUP IN THE U.S. WITH 95% C.I.

	R_0=1.5			R_0=1.8		
	IAR (%)	# of Infected*	# of deaths*	IAR (%)	# of Infected*	# of deaths*
<=19 yrs	28.74	27.41	10.96	38.43	36.65	14.66
	(26.65 - 30.82)	(25.42 - 29.39)	(10.17 - 11.76)	(35.7 - 41.15)	(34.05 - 39.25)	(13.62 - 15.70)
20-64 yrs	14.59	25.77	10.31	19.33	34.15	13.66
	(13.5 - 15.67)	(23.85 - 27.68)	(9.43 - 11.07)	(17.94 - 20.72)	(31.68 - 36.61)	(12.67 - 14.64)
65+ yrs	14.29	6.60	2.64	19.29	8.91	3.56
	(13.23 - 15.35)	(6.11 - 7.09)	(2.44 - 2.84)	(17.9 - 20.68)	(8.26 - 9.55)	(3.30 - 3.82)
Total U.S.	18.78	59.77	23.90	25.05	79.70	31.9
	(17.3 - 20.27)	(55.04 - 64.5)	(22.0 - 25.8)	(23.11 - 26.99)	(73.53 - 85.88)	(29.4 - 34.6)

* in millions

TABLE X

COMPARISON OF IARS AMONG DIFFERENT INFLUENZA VIRUSES

Description	H1N1 2009 (CDC)	H5N1 [7]	Seasonal Influenza	A(H7N9) (current paper)
Data used	Surveillance data from U.S. outbreak	Simulated outbreak in U.S. and England	Surveillance data from U.S.	Simulated outbreak in U.S.
Method used	Extrapolation with Correction factors	AB simulation model	Proposed by CDC [30]	AB simulation model and stratification
NPIs (school & workplace closure, case isolation)	yes (with antiviral)	yes (with vaccine and antivirals)	no	yes
Age-groups analysis	yes	yes	yes	yes
Estimated IAR	50%	28% for $R_0 = 1.7$ 34% for $R_0 = 2.0$	5% - 10% in adults 20% - 30% in children [29]	18.78% for $R_0 = 1.5$ 25.05% for $R_0 = 1.8$

VI DISCUSSION

Our paper is the first to estimate disease burden from A(H7N9) pandemic outbreak across the whole U.S., hence we could not directly compare our results with other A(H7N9) study. The disease parameter estimates used in our model were adopted from the recent reports on epidemiological studies of A(H7N9) [2, 9, 16, 29]. Other models (e.g., using differential equations) have been used to analyze A(H7N9) [28 – 30]. These models do not have the level of granularity of agent-based simulation models which can consider each individual in the population, their

household and age distribution, workplaces, schools and communities, daily schedule of activities, and travel behavior. However, such granularity comes with the cost of computation and memory usage, which resulted our model capacity to be limited to 5 million people per simulation run. We note that the limit can be increased with better computing hardware and more efficient usage of memory. Considering the five states that were selected for simulation, the 5 million limit only applied to California and New York. For the other three states, simulations were run for the whole urban population as the total population for each of these states are below 5 million. For California and New York, we used an agent-based proportional sampling approach to select up to 5 million individuals from the urban areas.

VII. CONCLUDING REMARKS

A recent paper in June 2016 [2] presented a comprehensive analysis of the laboratory-confirmed cases of A(H7N9) infection in mainland China. It presented renewed estimates for incubation period, fatality risk, hospital admission to death/discharge, median age, and poultry exposure. We note, however, that the parameter estimates that we used from an earlier study [16] do not differ significantly from those presented in [2]. Though it appears from the published data that A(H7N9) affects more people of higher age group, it is likely a function of the very high level of poultry exposure ($\geq$ 74% [16]) for the older age group. Our AB model does not incorporate any age-dependent factor for calculating probability of infection. However, our model does consider age-based contact process, which in turn affects the infection probability.

We simulated outbreaks only in urban areas and extrapolated the results to the population in the remaining (rural) areas. Urban areas constitute on average 3.4% of the geographic area and approximately 81% of the population [27]. Hence, the disease burden estimates, for each state, cluster, age-group as presented here, are likely to be upper bounds, as the population in rural areas are likely to be less affected. Also, applications of vaccines and antivirals were not considered in our AB model, which increased the number of susceptible and the intensity of infection, respectively. Furthermore, the disease burden estimates could have been lowered by application of the full extent of NPIs.

Our AB simulation model has the following notable limitations. It does not assign specific geographic locations for the households, places, and communities. As a result, we had to use estimated values for the distance between susceptible and infected $\left(f(d_{i,k}\right)$ in equation (1)) in calculating the force of infection. Use of antivirals could have reduced the profile of infectiousness with a lower peak and shorter duration reducing the virus spread and the corresponding IAR. Also, we did not consider pre-existing immunity for any age-group in the population.

VI. REFERENCES

[1] World Health Organization, “Summary and assessment, 20 december to 16 january 2017,” 2017, [Online; accessed 21-February-2017]. [Online]. Available: http://www.who.int/influenza/human_animal_interface/Influenza_Summary_IRA_HA_interface_01_16_2017_FINAL.pdf?ua=1

[2] P. Wu, Z. Peng, V. J. Fang, L. Feng, T. K. Tsang, H. Jiang, and et al., “Human infection with influenza a (h7n9) virus during 3 major epidemic waves, china, 2013–2015,” Emerging infectious diseases, vol. 22, no. 6, p. 964, 2016.

[3] Center for Disease Control and Prevention, “Avian influenza a(h7n9) virus,” 2016, [Online; accessed 7-June-2016]. [Online]. Available: fhttp://www.who.int/influenza/humananimal interface/influenza h7n9/en/g

[4] World Health Organization, “Cumulative number of confirmed human cases for avian influenza a(h5n1) reported to who, 2003-2016,” 2016, [Online; accessed 1-June-2016]. [Online]. Available: fhttp://www.who.int/influenza/human animal interface/EN GIP 20160509cumulativenumberH5N1cases.pdf?ua=1g

[5] World Health Organization, “Summary and assessment as of december 2015,” 2015, [Online; accessed 1-June-2016]. [Online]. Available: fhttp://www.who.int/influenza/ human animal interface/Influenza Summary IRA HA interface 14 Dec 2015.pdf?ua=1g

[6] N. M. Ferguson, D. A. Cummings, S. Cauchemez, C. Fraser, S. Riley, M. Aronrag, and et al., “Strategies for containing an emerging influenza pandemic in southeast asia,” Nature, vol. 437, no. 7056, pp. 209–214, 2005.

[7] N. M. Ferguson, D. A. Cummings, C. Fraser, J. C. Cajka, P. C. Cooley, and D. S. Burke, “Strategies for mitigating an influenza pandemic,” Nature, vol. 442, no. 7101, pp. 448–452, 2006.

[8] S. S. Shrestha, D. L. Swerdlow, R. H. Borse, V. S. Prabhu, L. Finelli, C. Y. Atkins, and et al., “Estimating the burden of 2009 pandemic influenza a (h1n1) in the united states (april 2009–april 2010),” Clinical Infectious Diseases, vol. 52, no. suppl 1, pp. S75–S82, 2011.

[9] Z. Liu and C.-T. Fang, “A modeling study of human infections with avian influenza a h7n9 virus in mainland china,” International Journal of Infectious Diseases, vol. 41, pp. 73–78, 2015.

[10] X. Zhou, Y. Li, Y. Wang, J. Edwards, F. Guo, A. C. Clements, and al., “The role of live poultry movement and live bird market biosecurity in the epidemiology of influenza a (h7n9):

A cross-sectional observational study in four eastern china provinces," Journal of Infection, vol. 71, no. 4, pp. 470–479, 2015.

[11] M. Husain, "Avian influenza a (h7n9) virus infection in humans: Epidemiology, evolution, and pathogenesis," Infection, Genetics and Evolution, vol. 28, pp. 304–312, 2014.
[12] V. K. Nguyen and E. A. Hernandez-Vargas, "Identifiability challenges in mathematical models of viral infectious diseases," IFACPapersOnLine, vol. 48, no. 28, pp. 257–262, 2015.

[13] T. Wang, "Dynamics of an epidemic model with spatial diffusion," Physica A: Statistical Mechanics and its Applications, vol. 409, pp. 119–129, 2014.

[14] J. Li, G.-Q. Sun, and Z. Jin, "Pattern formation of an epidemic model with time delay," Physica A: Statistical Mechanics and its Applications, vol. 403, pp. 100–109, 2014.

[15] L. N. Murillo, M. S. Murillo, and A. S. Perelson, "Towards multiscale modeling of influenza infection," Journal of theoretical biology, vol. 332, pp. 267–290, 2013.

[16] B. J. Cowling, L. Jin, E. H. Lau, Q. Liao, P. Wu, H. Jiang, and et al., "Comparative epidemiology of human infections with avian influenza a h7n9 and h5n1 viruses in china: a population-based study of laboratory confirmed cases," The Lancet, vol. 382, no. 9887, pp. 129–137, 2013.

[17] T. K. Das, A. A. Savachkin, and Y. Zhu, "A large-scale simulation model of pandemic influenza outbreaks for development of dynamic mitigation strategies," Iie Transactions, vol. 40, no. 9, pp. 893–905, 2008.

[18] A. Uribe-Sanchez, A. Savachkin, A. Santana, D. Prieto-Santa, and T. K. Das, "A predictive decision-aid methodology for dynamic mitigation of influenza pandemics," OR spectrum, vol. 33, no. 3, pp. 751–786, 2011.

[19] D. L. Martinez and T. K. Das, "Design of non-pharmaceutical intervention strategies for pandemic influenza outbreaks," BMC public health, vol. 14, no. 1, p. 1, 2014.

[20] D. Prieto and T. K. Das, "An operational epidemiological model for calibrating agent based simulations of pandemic influenza outbreaks," Health care management science, pp. 1–19, 2014.

[21] Prieto, D. M., Das, T. K., Savachkin, A., Uribe, A., Izurieta, R., and Malavade, S. 2012. A Systematic Review to Identify Areas of Enhancements of Pandemic Simulation Models for Higher Practical Usability. BMC Public Health 2012, 12:251,

[22] C. Reed, S. S. Chaves, P. D. Kirley, R. Emerson, D. Aragon, E. B. Hancock, and et al., "Estimating influenza disease burden from population-based surveillance data in the united states," PloS one, vol. 10, no. 3, p. e0118369, 2015.

[23] R. Scheaffer, W. Mendenhall III, R. Ott, and K. Gerow, Elementary survey sampling. Cengage Learning, 2011.

[24] National center for education statistics, “Number of public school districts, by locale code (ccd) and state: 2003-04,” 2003/04, [Online; accessed 21-May-2016]. [Online]. Available: fhttps://nces.ed.gov/surveys/ruraled/TablesHTML/5localedistricts.aspg

[25] United States Census Bureau, “Number of firms, number of establishments, employment, and annual payroll by enterprise employment size for the united states and states, totals: 2013,” 2013, [Online; accessed 21-May-2016]. [Online]. Available: fhttp://www.census.gov/econ/susb/g

[26] A. Hyder, D. L. Buckeridge, and B. Leung, “Predictive validation of an influenza spread model,” PloS one, vol. 8, no. 6, p. e65459, 2013.

[27] United States Census Bureau, “People residing in urban areas,” 2010, [Online; accessed 21-May-2016]. [Online]. Available: fhttps://ask.census.gov/faq.php?id=5000&faqId=5971g

[28] Kim, S., Lee, J., & Jung, E. Mathematical model of transmission dynamics and optimal control strategies for 2009 A/H1N1 influenza in the Republic of Korea. Journal of Theoretical Biology, 412, 74-85, 2017.

[29] Liu, Z., & Fang, C. T. A modeling study of human infections with avian influenza A H7N9 virus in mainland China. International Journal of Infectious Diseases, 41, 73-78, 2015.

[30] Chen, Y., & Wen, Y. Global dynamic analysis of a H7N9 avian-human influenza model in an outbreak region. Journal of theoretical biology, 367, 180-188, 2015

Appendix B: Analysis of the Infection Time during a Potential H7N9 Influenza Pandemic Outbreak

Analysis of the infection time during a potential H7N9 influenza pandemic outbreak

Walter Silva-Sotillo[1,2], MSc., Mingyang Li[2], PhD., Tapas K. Das[2], PhD.

[1]Pontificia Universidad Catolica del Peru, Peru, [2]University of South Florida, USA

silvasotillo@mail.usf.edu, mingyangli@usf.edu, das@usf.edu

Abstract

Avian influenza viruses have been affecting human populations for a long time since the outbreak in the year 1580 as the first recorded in history. Since then, other mutations and reassortments of the influenza viruses (e.g., H1N1, H3N2) have emerged causing pandemics. Recent emergence of H7N9 influenza virus in China has resulted in 1307 laboratory-confirmed cases of human infections causing 489 deaths (37.4% fatality rate). Researchers have developed early estimates of some of the epidemiological parameters to characterize H7N9 virus in China. In this research we examine the distribution that characterizes the time to infection from a potential H7N9 influenza pandemic outbreak using results from an agent-based (AB) simulation model. The AB model replicates the dynamics of contacts between susceptibles an infected individuals. We considered some of the common continuous probability distributions and conclude, based on the negative log-likelihood, that the lognormal distribution provides a good fit to characterize the time to be infected.

1 Introduction

AH7N9 is a subtype of influenza A virus that is found commonly in birds and poultry. Since March of 2013, A(H7N9) has been noted to infect humans in several regions of China, especially those who are in close contact with poultry either at farms or at markets dealing with poultry. So far, there has been five waves of infections since March 2013. A total of 1307 laboratory confirmed cases of A(H7N9) infections have been recorded in several regions of China causing 489 deaths [1]. The outbreaks have occurred in relatively densely populated regions of China that have over 54% of the country population. The average age of those infected in the first three waves have been reported to be 61, 57, and 56, respectively. However, the relative high age of those infected has not been attributed as an epidemiological characteristics of the A(H7N9) virus. Instead, it is conjectured to be a function of the higher level of exposure to poultry for elderly men in particular. Though most of the reported infections are known to be isolated cases of animal to human transmissions, researchers have noted exceptions where they believe human-to-human transmission may have occurred. However, it is concluded that there is still a lack of sustained evidence of human-to-human transmission [2].

It is feared though that A(H7N9) influenza virus could gain the ability to mutate or reassort to become human-to-human transmittable and cause a pandemic. Similar situation happened with H5N1 during the years 2003-2009 where scientists believed that H5N1 was highly likely to become human-to-human transmittable and cause a pandemic. Though an H5N1 pandemic did not occur as yet, this virus is still in circulation and, as reported by WHO, has caused 145 infections and 42 deaths in three countries in 2015 [3].

An important observation made so far about A(H7N9) is that, though it is highly pathogenic both in humans and birds, infected poultry remain asymptomatic and do not die. This makes it difficult to identify the spread of A(H7N9) among poultry. In recent years, the Chinese government has applied containment measures to limit the spread of the virus including culling birds and closing live poultry-

markets and trading areas.

The objective of the research underlying the content of this paper was to characterize the infection time for a potential A(H7N9) influenza pandemic outbreak. We used data from recent reports and an updated version of our previously developed AB simulation model [4, 5, 6] to simulate an outbreak and estimate which distribution provides better understanding of the time to be infected. The simulation model replicates the dynamics of pandemic outbreak in a selected area incorporating the demographic information (households, schools, workplaces, and communities), human behavior (including contacts, compliance to quarantine and other public health measures, and travel), epidemiological parameters of the virus (e.g., force of infection, incubation and latent periods, basic reproduction number (R_0), and fatality rate), and non-pharmaceutical intervention strategies (NPI) for containment and mitigation. The AB model considers detailed information about the households and their member compositions (age, sex, work, parental status), distance between individuals and their daily movements, contact processes, infection process, and disease natural history. We assumed that during the outbreaks, an *ad-hoc* or an *optimal* NPI strategy (which was found as optimal for a generic influenza virus) was in place with a goal to contain the spread. The NPI strategy comprised measures like isolation, quarantine, school and workplace closures.

The remaining part of the paper is organized as follows. In Section 2, we describe the methods used in this research. Section 3 presents the results. Section 4 outlines the conclusions and Section 5 discusses important points from this research and propose future work.

2 Methods

In this section we will describe the disease natural history, the AB simulation model, the interventions and the statistical modeling of the infection time.

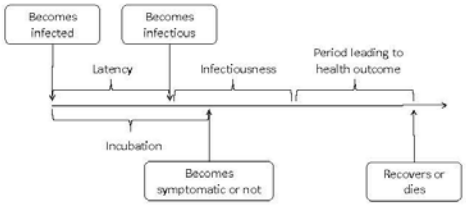

Figure 1: Typical influenza disease natural history showing the progression of the disease from the moment of exposure until health outcome.

Once a person becomes infected, s/he starts a period of latency. During this period, infected individuals cannot infect other persons. After this, the person becomes infectious and can spread virus to susceptibles individuals in a symptomatic or asymptomatic way which is defined by the incubation period. Finally, after the infectiousness period is over the person either recovers and becomes immune or dies. Figure 1 describes the influenza disease natural history. That schema is used in the AB model to simulate the contact and infection process for each individual.

2.1 Agent-based simulation model

The agent-based (AB) simulation model provides output data to be used to analyze the behavior of the time to be infected. Figure 2 depicts the process used in the AB model. Individuals and households are generated and associated. Then schools, workplaces, community locations and schedules are also assigned to the persons. After generating all population, some infected individuals are released in the model to trigger a pandemic. The model keeps daily trace of susceptible and infected individuals and checks for contacts in households, workplaces/schools and community places.

By the end of the day, the model calculates the force of infection for each susceptible individual, cal-

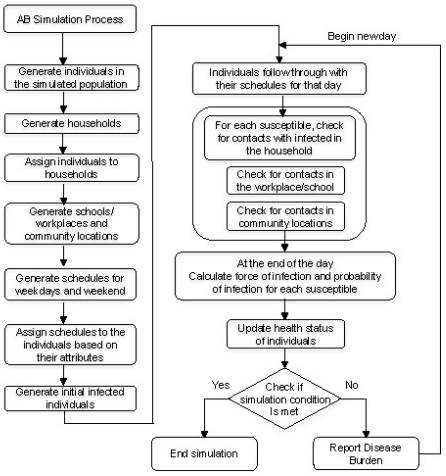

Figure 2: Schematic of the AB model.

culates the probability of infection and update the health status for each susceptibles person. After having no more infected and reaching the simulation condition the model stops and generates output files containing relevant daily statistics (e.g.,number of infected persons, number of deaths, number of persons that visit the doctor, number of persons recovered, etc.).

2.2 Non-pharmaceutical interventions

We assume that during an outbreak, a NPI strategy will be in place with a goal to contain the spread (that is, to keep the reproduction number $R_0 < 1$ and infection attack rate $IAR < 0.1$). A NPI strategy comprises measures like social distancing, isolation, quarantine, school and workplace closure, and travel restrictions. Consequently, there can be numerous possible strategies based on the chosen parameter values for the measures. We implement two NPIs strategies, one *ad-hoc* and the other that was recommended in [5]. We refer to the strategies as NPI(1) and NPI(2). Table 1 shows the 16 factors involved in the NPI and their corresponding values used in the AB model.

Global thresold is associated with the number of cases needed to declare an outbreak of influenza. *Deployment Delay* is the time needed to fully deploy NPIs after the onset of an outbreak. *Case isolation* is related to isolate an infected individual at home. *Household quarantine* measures the restriction to leave the house to the household members of an infected person. *School closure* defines the number of students infected in a class to close a class, the number of classes closed to close a school and the duration of such closure. *Workplace closure* requires the number of cases to close a department in a workplace, the percentage of departments closed to close the workplace and the duration of the workplace closure.

Factor	Intervention	NPI(1)	NPI(2)
1	Global Threshold	10	10
2	Deployment delay	3 days	7 days
3	Case isolation threshold	1 day	1 day
4	Case isolation duration	7 days	10 days
5	Case isolation compliance for workers	75%	75%
6	Case isolation compliance for non-workers	84%	87%
7	Household quarantine threshold	1 day	1 day
8	Household quarantine duration	7 days	7 days
9	Household quarantine compliance workers	75%	53%
10	Household quarantine compliance non-workers	84%	84%
11	Cases to close a class in a school	4	1
12	Classes to close a school	6	3
13	School closure duration	10 days	21 days
14	# cases to close a department in a workplace	6	3
15	% of departments to close a workplace	60%	30%
16	Workplace closure duration	10 days	7 days

Table 1: Parameters for two NPI strategies

2.3 Statistical modeling of infection time

Due to the right-skewness of infection time data, in this section, we investigated different survival distributions, such as exponential, weibull and

log-normal, to characterize the time to infection data. The last two distributions are more flexible in representing the various heavy-tailed infection time data. All results are implemented in the statistical computing environment of *R* software [7, 8].

The maximum likelihood estimation (MLE) is employed to estimate the distribution parameters by maximizing the data likelihood (LIK) function described below:

$$LIK = [F(t_1)^{r_1}]\{\prod_{i=2}^{m}[F(t_i) - F(t_{i-1})]^{r_i}\} \quad (1)$$

where $F(t_i)$ is the cumulative number of infected persons up to time i, r_i is the number of infections in interval i, n is the total number of infected persons and m is the day when there is no more infected individuals. In our case, m can vary depending on the scenario evaluated and our analysis of infections considers only days with infected persons.

2.3.1 Exponential distribution

The exponential distribution is the simplest distribution in the analysis of reliability/survival data and has a constant hazard. *Start* and *end* are the starting and ending interval time respectively (see Section 2.4 for more detail). Totlife is defined as the time elapsed before getting infected.

$$Totlife = \sum_{t}((start + end)/2 * infected) \quad (2)$$

The exponential hazard rate (i.e., the instantaneous probability of being infected) and the corresponding mean time to be infected (MTTI) are presented in equations 3 and 4.

$$\lambda = \sum_{t}(infected/Totlife) \quad (3)$$

$$MTTI = 1/\lambda \quad (4)$$

2.3.2 Weibull distribution

Weibull distribution is a generalization of the exponential distribution and is often used in biomedical applications. It can be used to model infection data with a decreasing, a constant or an increasing hazard rate.

Based on the MLE, distribution parameters of weibull, namely the rate parameter α and the shape parameter β, can be simultaneously estimated. The correponding MTTI is given by,

$$MTTI = \alpha\Gamma(1 + 1/\beta) \quad (5)$$

2.3.3 Lognormal distribution

The lognormal distribution offers flexible shapes for the probability density functions (pdfs) and hazard rate functions. This distribution is preferred when there is a hypothetical multiplicative and progressive increments that could trigger a critical event, e.g., the ocurrence of infection. In the context of pandemic outbreaks, such progressive increments can be interpreted as the increasing number of infections during the first days of pandemics. This means also an increasing number of contacts that a susceptible individual faces which feeds the amount of virus ingested and hence, it affects the probability of getting infected.

If $T \sim lognormal(T_{50}, \sigma)$, then $lnT \sim N(lnT_{50}, \sigma)$, where T_{50} is the median infection time for the population of lognormal infection time observations and σ is the standard deviation of the logarithmic transformation of infection times (i.e., shape parameter). Equivalent, if $X \sim N(\mu, \sigma)$, then $e^X \sim lognormal(e^\mu, \sigma)$. Both parameters can be estimated as follows.

$$T_{50} = e^\mu \quad (6)$$

$$\sigma = ln(e^{\sigma\phi^{-1}F(t)})/(\phi^{-1}F(t)) \quad (7)$$

where $F(t)$ is the cumulative distribution function (cdf) of the lognormal distribution. The MTTF is estimated from:

$$MTTI = T_{50} e^{\sigma^2/\mu} \tag{8}$$

2.4 Problem description and data

The data comes from the AB model that use epidemiological information from H7N9 outbreak in China and combined that with U.S. demographical parameters to replicate a potential H7N9 outbreak in the U.S. One of the outputs of the AB simulation model is the daily number of infected persons which is used in this study. This value is considered up to the day where no further infections are detected.

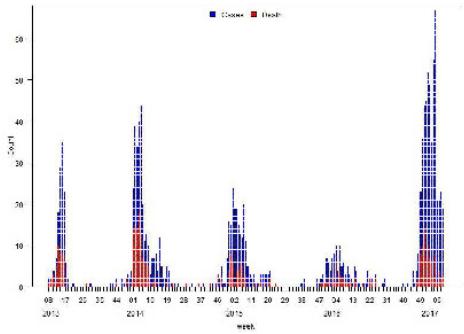

Figure 3: Laboratory-confirmed cases and deaths of human infection with A(H7N9) reported by WHO.

The data used in this research was simulated for a population of 1.27 million of persons (Hillsborough county area in Tampa Bay) considering a moderate force of infection. The number of incidences of H7N9 in China has been reducing since 2013 but researchers think that a potential pandemic can occur at any time and more dangerous is that the virus mutate or reassort to a human-to-human transmittable. Figure 3 shows the number of cases since initial outbreak.

We used readout data consisting of *interval*, *start*, *end* and *infected*. This data is obtained from the AB model output report and is used in the three statistical distributions proposed.

Finally, this study considers 6 scenarios associated with the variation on the NPI used (as described in section 2.2) and the potential force of spread which is related with the IAR, beeing 33%, 50% and 65% the values more considered in the literature.

3 Results

In the present project we considered three main distributions as potential candidates to describe the time to infection from an influenza pandemic outbreak: exponential, weibull and log-normal. After running the AB model, we obtained as output the daily number of infected cases. This information is used as readout data to proceed estimating the main parameters, the LIK and the MTTI for each case.

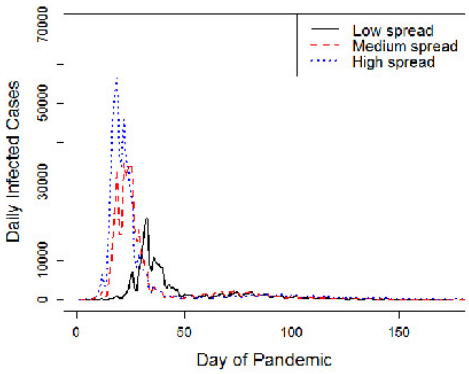

Figure 4: Simulated daily infected cases for NPI(1).

Simulated infected cases are shown in figure 4 and figure 5 for NPI(1) and NPI(2) respectively and for the three levels of spread. From figure 3, for a given

year, each one of the waves displayed seems not to differ significantly from the shape obtained as result from our AB simulation model depicted in figures 4 and 5. It is important to notice that in figure 5, we observe the presence of waves in all spread cases. Our procedure takes in consideration all time frame, hence all waves in the estimations. Parameters estimated for the exponential (λ), weibull (α, β) and lognormal (T_{50}, σ) distributions are respectively displayed in Table 2 for NPI(1) and in Table 3 for NPI(2).

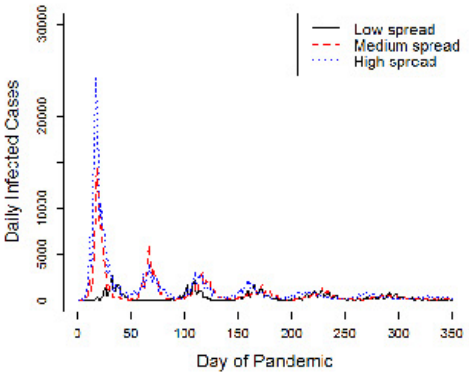

Figure 5: Simulated daily infected cases for NPI(2).

Spread	Distribution	Parameters	MTTI	LIK
Low	Exponential	0.00069	1440.05	-1429.40
	Weibull	(707.99,0.51)	1366.07	-1343.747
	Lognormal	(5.51,2.21)	96.40	-1342.92
Medium	Exponential	0.00038	2642.62	-1607.19
	Weibull	(978.35,0.47)	2208.31	-1462.15
	Lognormal	(5.80,2.67)	334.72	-1455.18
High	Exponential	0.00036	2794.97	-1992.63
	Weibull	(866.38,0.46)	2046.32	-1777.91
	Lognormal	(5.69,2.26)	107.37	-1765.95

Table 2: Estimated parameters for each distribution and for each force of spread when NPI(1) is deployed.

Spread	Distribution	Parameters	MTTI	LIK
Low	Exponential	0.00270	369.46	-2419.22
	Weibull	(338.52,0.85)	368.29	-2410.31
	Lognormal	(5.16,1.39)	16.75	-2418.44
Medium	Exponential	0.001135	880.82	-2723.30
	Weibull	(727.24,0.81)	846.77	-2706.31
	Lognormal	(6.06,1.08)	11.58	-2646.97
High	Exponential	0.000785	1273.83	-2852.42
	Weibull	(1039.47,0.81)	1167.44	-2824.98
	Lognormal	(6.45,1.03)	11.39	-2766.91

Table 3: Estimated parameters for each distribution and for each force of spread when NPI(2) is deployed.

4 Discussion

To estimate the distribution parameters of the mentioned three distributions, maximum likelihood function in (1) is maximized based on numerical optimization methods. For exponential distribution, single parameter is estimated based on the $Nelder-Mead$ method [9]. For Weibull and Lognormal distributions, $Broyden-Fletcher-Goldfarb$ and $Shanno$ (BFGS) method [10] is considered to estimate the two-dimensional parameters. The estimation results for three parametric survival distributions are implemented via *fitdistr* function in *R*.

The negative log-likelihood (LIK) is considered as the goodness-of-fit measure to evaluate and compare the performance among different distributions. A smaller value of LIK indicates a better goodness-of-fit. Among all 6 scenarios, Exponential distribution gives the largest LIK values and thus exhibits the poorest goodness-of-fit. It is mainly due to its less flexibility in representing different shapes of infection data.

As depicted in table 3, the weibull distribution outperforms other distribution with better goodness-of-fit in the low spread scenario. However, its corresponding LIK value is not far away from its counterpart of lognormal distribution. As shown in all scenarios, the estimated shape parameters of weibull distribution is less than 1. It implies a decreasing hazard rate over time. In the context of

pandemic outbreak, it indicates that the infection rate is decreasing over time and eventually the pandemic will stop. The estimation results of weibull distribution also explain the reason why exponential distribution exhibits unsatisfactory goodness-of-fit. In exponential distribution, hazard rate is constant. It indicates that the inflection rate will not change over time, which fails the capture the actual pandemic outbreak process with dynamically changing inflection rate.

Among 5 out of 6 scenarios, lognormal distribution gives the most superior performance of goodness of-fit. There are mainly two reasons. From the data fitting perspective, comparing to weibull distribution, lognormal distribution has similar capability and flexibility to represent various heavy tails and right-skewed inflection time data. From the pandemic outbreak process perspective, lognormal distribution can more closely mimic the underlying process, and thus gives satisfactory results. In addition, it is noticed that goodness-of-fit results of weibull and lognormal distributions are similar and lognormal exhibits slightly better results. The hazard rate of lognormal is in complex form and less interpretable compared to weibull distribution. Thus, weibull distribution is still valuable in providing compact and interpretable information (e.g., decreasing infection rate) while maintaining a reasonable well goodness-of-fit of data.

5 Conclusion and future work

An inconvenient for this study is that we do not have the exact time of infection but just the number of people infected daily. Having more detailed information from official sources (e.g., CDC, CDC China, WHO) could help to: i) expand the study including time of death and time of recovery, and ii) have better estimates.

Another important improvement to consider is to disaggregate the analysis (infected and deaths) according to age groups: $< 19yrs$, $20 - 64yrs$ and $65 + yrs$. This could help to the making decision process since H7N9 attacks mainly elder people ($65 + yrs$ group). and other influenza viruses can have different age-targets.

It is also known that not all infected persons are symptomatic and a significant part of the population can stay as asymptomatic (they don't show symptoms, hence they don't know that they are sick). Official reports do not capture those asymptomatic cases that may affect our estimations. We propose to develop some multipliers and incorporate them to better estimate the number of infected persons and to capture the real nature of the infection process.

Finally, as seen in figure 5, distribution of number of infected persons exhibit multi-modal shapes at different waves and none of the proposed distributions can capture the real nature of that behavior. We will address this issue in details by investigating mixture distributions and their variants in the future.

References

[1] World Health Organization, "Summary and assessment, 14 february to 16 march 2017," 2017. [Online; accessed 31-March-2017].

[2] World Health Organization, "Analysis of recent scientific information on avian influenza a(h7n9) virus," 2017. [Online; accessed 11-April-2017].

[3] World Health Organization, "Cumulative number of confirmed human cases for avian influenza a(h5n1) reported to who, 2003-2016," 2016. [Online; accessed 21-April-2017].

[4] A. Uribe-Sánchez, A. Savachkin, A. Santana, D. Prieto-Santa, and T. K. Das, "A predictive decision-aid methodology for dynamic mitigation of influenza pandemics," *OR spectrum*, vol. 33, no. 3, pp. 751–786, 2011.

[5] D. L. Martinez and T. K. Das, "Design of non-pharmaceutical intervention strategies for pandemic influenza outbreaks," *BMC public health*, vol. 14, no. 1, p. 1, 2014.

[6] T. K. Das, A. A. Savachkin, and Y. Zhu, "A large-scale simulation model of pandemic influenza outbreaks for development of dynamic mitigation strategies," *Iie Transactions*, vol. 40, no. 9, pp. 893–905, 2008.

[7] Marie Laure Delignette-Muller, Christophe Dutang, "An r package for fitting distributions," 2014. [Online; accessed 30-March-2017].

[8] Vito Ricci, "Fitting distributions with r," 2005. [Online; accessed 30-March-2017].

[9] J. A. Nelder and R. Mead, "A simplex method for function minimization," *The computer journal*, vol. 7, no. 4, pp. 308–313, 1965.

[10] D. F. Shanno, "Conditioning of quasi-newton methods for function minimization," *Mathematics of computation*, vol. 24, no. 111, pp. 647–656, 1970.

Appendix C: Resilience as a Measure of Preparedness for Pandemic Influenza Outbreaks

Resilience as a Measure of Preparedness for Pandemic Influenza Outbreaks

Walter Silva-Sotillo*, Daniel Romero-Rodriguez, Alex Savachkin, Tapas K. Das

University of South Florida, Department of Industrial Management and Systems Engineering

Abstract

Periodic emergence of avian influenza A(H7N9) virus in China has heightened concerns for a possible pandemic outbreak. From a public health preparedness standpoint, it is essential to measure the capability of the affected communities to withstand and recover quickly from a pandemic outbreak. This property is known as resilience. The aim of this research is to develop community resilience measures and demonstrate their estimation using a simulated pandemic outbreak in a region in the U.S. with a relatively large population. Three scenarios are analyzed with different combinations of virus transmissibility rates and non-pharmaceutical interventions. The agent-based simulation model replicates human interactions, spread of infection and resulting impact on human lives and society. The average percentage of healthy population at any point in time is used to quantify resilience. In addition, a relative resilience metric based on the performance loss function is proposed. This new metric is used to show that resilience is improved between 1.82 and 7.25 times when recommended NPIs are deployed.

1 Introduction

Influenza ranks among the most common viral infections. Infection spreads when susceptible individuals are in contact with infected animals or persons. The result of infection is often fatal for senior adults and children. The center for disease control and prevention (CDC) estimates that for the 2015-2016 season, vaccination in the U.S. has prevented around 5.1 million influenza illnesses, 2.5 million influenza-associated medical visits and 71,000 influenza-associated hospitalizations. In the other hand, the burden of influenza in 2015-16 was estimated to be 25 million illnesses, 11 million medical visits, 310,000 hospitalizations, and 12,000 cases of pneumonia and influenza inflicted deaths [1].

Main strains of influenza viruses are currently in circulation, e.g., H7N9 (China), H1N1 (worldwide), H5N1 (worldwide). A(H7N9) is a subtype of influenza A virus that is found in birds including poultry. Since March of 2013, A(H7N9) has been noted to infect humans in several regions of China, especially those who are in close contact with poultry either at farms or at markets dealing with poultry. So far, there have been four waves of infections in spring of 2013 and winters of 2013-14, 2014-15 and 2015-16. The fifth wave of infections is currently in progress. Since spring 2013 till March 2017, a total of 1307 laboratory-confirmed cases of A(H7N9) infections have been recorded in different regions of China causing at least 489 deaths (37.4% fatality rate) [2]. It has also been noted in the literature that the high exposure to infected poultry contributed to the elders more infected than other age-groups. Though most of the infections are confirmed to be animal-to-human transmitted, researchers believe that some cases may have been human-to-human transmitted. However, current epidemiological and virological evidence suggests that this virus has not acquired the ability of sustained transmission among humans [3]. Apprehension of A(H7N9) showed that it might gain the ability to mutate or reassort to become human-to-human transmittable and cause a pandemic. Hence, it is important to be able to assess the level of resilience of the mitigation measure that are available to assess the possible impact and to measure how to protect the population from

a pandemic outbreak. Readers may recall that there was a significant fear of a H5N1 influenza pandemic outbreak during the years 2003-2009, and till date, the virus has infected a total of 858 people worldwide, of which 453 are dead (52.8% fatality rate) [2]. The fear of H5N1 pandemic triggered research studies published in 2005 [4] and 2006 [5], which critically examined the impact of potential H5N1 outbreaks in Thailand and jointly in the U.S. and UK, respectively. Though an H5N1 pandemic did not occur as yet, this avian influenza virus is still in circulation and is still causing deaths, as reported by WHO [6]. In 2009, Influenza H1N1 attacked worldwide including the U.S., where the burden has been estimated to be 60.8 million of infections and 12,469 deaths [7].

Though the impact of influenza pandemic outbreaks is generally measured via the numbers of infections and deaths, their impact on the economic activities, education and overall healthcare delivery can be very significant. Such negative impacts also arise from natural disasters affecting infrastructure and communities by disrupting interconnected systems and generating high death tolls and economical losses [8]. In case of influenza pandemic outbreaks, even though physical infrastructure is not impacted directly, they disrupt the workforce availability leading to reduced productivity [9]. In order to avoid or minimize the effects of pandemic outbreaks, communities thus should make mitigation plans to improve their resilience. The importance of community resilience has been highlighted by the CDC, which defined it as *"the ability to prevent, withstand and recover from public health incidents"* [10].

Traditionally, the impact of pandemic outbreaks preparedness has been measured using the infection attack rate (IAR) [11, 12]. This metric quantifies the total percentage of infected individuals in a population by the end of an outbreak. Resilience is a multivariate measure and thus a more adequate tool to estimate a community's ability to cope with a pandemic outbreak.

The measure of community or social resilience is defined incorporating different capacities: absorptive and restorative [13, 14]. In the context of influenza pandemics, the absorptive capacity is characterized by the number of infected people, and the restorative capacity is measured by the time to recover. Therefore, the goal of a resilient community is to minimize a joint measure, the extent of infected population and the recovery time.

Resiliency is a key attribute of any system to preserve and improve performance outcomes throughout the period of adversities. This has led to the exploration and implementation of this concept in different areas of study. Its introduction since 1973 [16], the concept of resilience has been adopted, in engineering [17], psychology [18], economics [19], ecology [20], management [21] among others. However, in the open literature and in the analysis of pandemics influenza outbreaks, resilience has not been introduced as a measure of performance. Also, there is no commonly accepted model or approach to measure resilience, and hence it is assessed using different qualitative and quantitative tools [22]. In this research, we review the available quantitative metrics with a goal to using them to assess the impact of different system interventions or policies during a pandemic outbreak. The metrics are classified in two categories: the multiple indexes and the average performance metrics.

In the first group, a wide variety of indices are combined to express a system's resilience level [23]. One such resilience model is the multiplication of three individual metrics that capture absorptive, restorative and adaptive capacities [24]. Composite metrics are developed via different methodologies that combine social, economical and environmental factors to explore multiple dimensions [25, 26]. In the second category, we discuss the average performance (or, the resilience triangle) metrics the first of which was introduced in [27] in the context of community resilience under seismic events. Average performance metric captures both the absorptive and restorative capacities. This metric paradigm has been subsequently modified to fit linear responses

[28], non-linear performance functions [29], multiple disruptions [30], stochastic parameters [31] and time dependent metrics [32]. The popularity of this approach resides in the interpretability and ease of use in evaluating strategies to improve a system's resilience.

Resilience was used as a measure to develop communication management strategies during events like eartquakes, flu, and terrorism [33]. To our knowledge, our work as presented in this paper is the first formal effort to evaluate the impact of non-pharmaceutical interventions (NPIs) on a community's resilience levels during an influenza pandemic.

The remaining sections of this paper are as follows. Section 2 describes the methods and metrics that are implemented to assess resilience, as well as the agent based simulation test bed used in this study. Section 3 explores the simulation results and the corresponding resilience measures. In Section 4, the results are used to identify the pros and cons of the methods proposed in this paper to study community resilience under pandemic outbreaks. Finally, in Section 5 the contribution of the resilience framework in healthcare is highlighted and future research areas are identified.

2 Methods

In this study, we have used a recent version of an agent-based (AB) simulation model that was developed in our previous studies of influenza pandemic [34, 35, 36]. The AB model replicates an influenza pandemic outbreak considering epidemiological parameters (e.g., incubation and latent period, force of infection); demographic information about the population (e.g., household members and their age, sex, parental status, distance between infected and susceptible individuals), infection process, contact process and disease natural history.

Our study considers different potential virus transmissibility scenarios as well as different types and extent of non-pharmaceutical interventions (NPIs) including isolation, household quarantine, school and workplace closure.

We execute the AB model for the various combinations of the virus transmissibility rates and the intervention methods. The runs of the model generates the infection pattern as well as the attack rates, which are used to estimate resilience.

2.1 AB simulation model

The AB model begins by generating individuals and their designated households (see Figure 1) in the outbreak region. The model thereafter generates schools, workplaces and communities, and the daily activity schedules suitables for various types of individuals. The model initiates the ourbreak by releasing some infected individuals in the population and keep track till the end of each day of the status of each person. Susceptibles who come in contact with infected individuals gather force of infection, the levels of which are used to determine if the susceptibles become infected. The infected follow through a disease natural history and either recover and become immune or die.

The AB model considers three NPIs scenarios: first, where no interventions are applied; second, where an arbitrary set of NPIs as in [37] are used; and the third considers an optimal NPI as in [36]. Three intervention scenarios and three virus transmissibility rates are combined into nine cases. for each case, the output summary file contains relevant information including *number of infected*, *number of recovered*, and *number of deceased*.

2.2 Interventions

Mitigation containtment strategies for pandemic influenza include both pharmaceutical and non pharmaceutical interventions (PI and NPI). The PI includes vaccines and antivirals. Vaccines usually take several months to develop, produce, and distribute. The level of stockpile of antivirals at the time of an influenza pandemic outbreak be

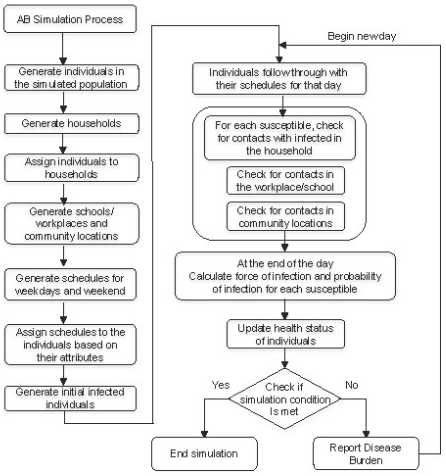

Figure 1: AB simulation model

limited. Moreover, antivirals don't praide immunity from infection but can reduce the severity of the infection. The NPIs include social distancing, household quarantine, isolation, school and workplace closure. These measures are easy to apply and can be executed at early stages of the pandemic outbreak. For this study, we consider only the use of NPIs. In under resourced countries, this is the best available measure to apply due to the unavailability of vaccines and antivirals. Another advantage of using NPIs is that they can provide the first line of defense before vaccines are developed.

In this study, we applied a set of NPIs with certain parameter combinations that were recommended in [36] as shown in Table 1 (NPI (2)). For the purpose of comparison, we also implemented another NPI with somewhat random set of parameters. These interventions are supposed to act as a containment measure for the spread of virus.

#	Measure	NPI (1)	NPI (2)
1	Global Threshold	10	10
2	Deployment delay	3 days	7 days
3	Case isolation threshold	1 day	1 day
4	Case isolation duration	7 days	10 days
5	Case isolation compliance for workers	75%	75%
6	Case isolation compliance for non-workers	84%	57%
7	Household quarantine threshold	1 day	1 day
8	Household quarantine duration	7 days	7 days
9	Household quarantine compliance workers	75%	53%
10	Household quarantine compliance non-workers	84%	84%
11	Cases to close a class in a school	4	1
12	Classes to close a school	6	3
13	School closure duration	10 days	21 days
14	# cases to close a department in a workplace	6	3
15	% of departments to close a workplace	60%	30%
16	Workplace closure duration	10 days	7 days

Table 1: NPI parameters

Global thresold refers to the number of cases needed to declare an outbreak of influenza. *Deployment Delay* is the time needed to fully deploy NPIs after the onset of an outbreak. *Case isolation* is the time that an infected individual should stay at home. *Household quarantine* is related to the restriction of movement of household members of an infected case (not the infected case). *School closure* requires number of infected students in a class and number of classes infected in a school to close the class and the school, respectively. *Workplace closure* is similar to school closure but consider workplaces instead of schools.

2.3 Test bed data

For this study we simulated an outbreak region with a population of 1.2 million people. The epidemiological parameters (e.g., force of infection, incubation and latent periods, basic reproduction number, and fatality rate) were estimated from the recent studies on H7N9 influenza outbreak in China. The U.S. census and travel data were used for households, schools, workplaces, communities, and human behavior (e.g., contacts, compliance to isolation).

2.4 Measuring resilience

The approaches we have selected to quantify resilience levels is via measure of the cumulative loss

function. This metric considers the key dimensions of number of infected people and the recovery time. Another key feature of this metric is the simplicity to be operationalized in a simulation model. In contrast, composite indices require multiple indicators that can not be modeled easily to capture potential changes in the system's policies.

We define the fraction of the healthy population at any time t as $H(t)$, where $I(t)$ denotes the number of infected at time t, $R(t)$ and $D(t)$ represent the number of recovered and the number of deceased, respectively.

$$H(t) = \frac{H(t-1) - I(t) + R(t)}{Population - \int_0^T D(t)} \tag{1}$$

The value of $TH(t)$ throughout the resilience analysis is 100% and T_f represents the study time. We also define the loss function L as the cumulative difference between the desired level of healthy population (denoted as $TH(t)$) and the actual level $H(t)$ over the total duration of a pandemic (T_f). We write this as

$$L = \int_{t_0}^{T_f} (TH(t) - H(t))dt, \tag{2}$$

where t_0 is the start time of a pandemic. Let $H^*(t)$ denote the percentage of healthy population when the best available intervention policy is implemented. We define a resilience measure for policy performance comparison as

$$R = \frac{\int_{t_0}^{T_f} (TH(t) - H^*(t))dt}{\int_{t_0}^{T_f} (TH(t) - H(t))dt}. \tag{3}$$

In addition to the resilience measures L and R, we have used in our analysis two other related measures: X (initial drop in $H(t)$) and T(the duration of a pandemic till the percentage of infected is less than 1%).

3 Results

The interpretation of the metrics X, T and L provides a general idea of the different types of community resiliency levels.

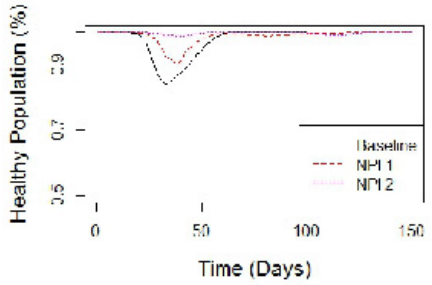

Figure 2: Daily % of healthy population in the low transmissibility rate scenario

X measures the maximum drop in $H(t)$. Thus smaller the value of X higher the absorptive capacity. The variable T represents how quickly the system is restored to the initial or desired state. Clearly for T, it is smaller the better. The value of L includes both variables (X and T) in estimating the resilience.

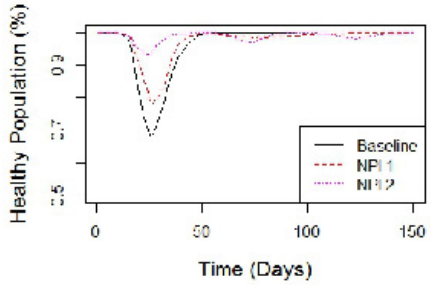

Figure 3: Daily % of healthy population in the medium transmissibility rate scenario

The scenarios comparison is divided based on the

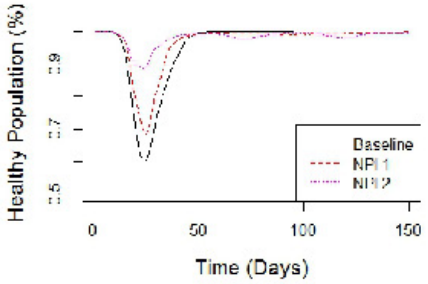

Figure 4: Daily % of healthy population in the high transmissibility rate scenario

transmissibility rate. Figures 2, 3 and 4 depict the daily % of healthy population in the low, medium, and high transmissibility rate cases respectively. Table 2 shows the resilience levels summary for all scenarios. A predominant observation made from Table 2 is that the cumulative loss L is smaller in the best available NPI policy regardless of the transmissibility rate.

IAR	Policy	$X(\%)$	T	L	R
	Baseline	16.00	49	3.01	0.137
Low	NPI (1)	9.49	114	1.95	0.232
	NPI (2)	1.34	36	0.45	-
	Baseline	31.62	48	5.05	0.344
Medium	NPI (1)	21.61	127	3.73	0.466
	NPI (2)	6.71	127	1.74	-
	Baseline	39.97	49	6.45	0.409
High	NPI (1)	31.30	158	4.83	0.547
	NPI (2)	11.26	158	2.64	-

Table 2: IAR (transmissibility) comparison and estimated resilience levels

In the analysis of all the transmissibility scenarios from Table 2, the metrics L and X are better when NPIs are implemented for low transmissibility rates. For T, the behavior was not as expected due to non-linearities of the responses, which are discussed in more details in the next section.

Figure 5 depicts the daily cumulative loss in the high transmissibility rate case.

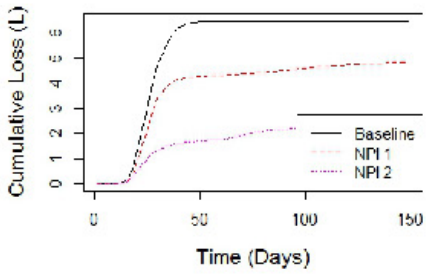

Figure 5: Daily cumulative Loss in the high transmissibility scenario

4 Discussion

The benefits of NPI are evident from the resilience measures. We note that the value of X is reduced in both NPI(1) and NPI(2). This result suggests that the absorptive capacity is improved. In the case of the response variable T, the situation is not the same because the recovery time increased significantly for the medium and high attack rates. Even though the overall system resilience (L) is enhanced by the static resilience (X), the dynamic counterpart (T) is affected.

This could be due to the fact that in both NPI scenarios after the day 50 there are infection waves where the number of infected people increases but not up to the levels of the first wave. Although the overall number of infected people is lower during the first wave in the NPI scenarios, when the virus

reemerges, less people are susceptible to get infected. In the baseline scenario since most of the population is infected in the first wave, even less people are affected in the subsequent outbreaks.

The presence of multiple outbreaks or infection waves are part of the Influenza virus normal pattern [38]. This behavior has been documented in the resilience literature as the multi-disruption scenario, where natural disasters such as earthquakes disrupt a community multiple times in waves or replicas [30, 39]. The mitigation of the upcoming waves requires that policies should be designed to minimize X and T. This suggestion can be performed by evaluating the potential impact of the implementation of dynamic NPIs or PIs (Pharmaceutical interventions) that may reduce the probability of getting infected in any of the expected outbreaks subsequent to the first one.

The comparison of scenarios was carried out with the relative resilience ratio metric, but it is possible to test and compare alternative metrics that could include additional dimensions or different interpretations. The insights provided by the resilience framework applied to the pandemics analysis are beneficial to enabling a broader understanding of community prevention and recovery capacities.

Our study considers epidemiological parameters from A(H7N9) influenza outbreak in China and uses demographic parameters from U.S. This virus is not yet human-to-human transmittable, however, it is important to highlight the following aspects: 1) the potential damage that a mutation or reassortment of this virus could trigger is considered in this study, and 2) the epidemiological parameters that are used with their corresponding confidence intervals do not differ significantly from the parameters of other influenza viruses. Hence, this study is not limited to A(H7N9) and can be broadly applied for other influenza viruses.

5 Conclusions

Use of NPI increased community resilience during influenza pandemic outbreaks from viruses with low, medium and high transsmisibility rates. The overall improvement was generated by the absorptive capacity (X), even though the restorative capacity (T) worsened for the medium and and high transmissibility rate scenarios.

The inclusion of the resilience framework in the pandemic analysis enriches the discussion in how to design effective intervention strategies to prevent, mitigate and recover from a potential influenza pandemic outbreak. The ability to capture multiple dimensions encapsulated in the resilience concept provides an integrative approach to enhance system response capabilities.

The AB simulation model provides the estimates for the healthy population, key measure used to describe our resilience metric. However, other measures may also been relevant to assess resilience, such as number of visits to the doctor, number of hours of school abscense, and lost of work productivity.

Future research in this area will require to explore the following aspects: i) resilience metrics comparison, ii) pharmaceutical interventions (PIs) and dynamic strategies, and iii) different virus and demographics. The evaluation of alternative resilience metrics is suggested to include dimensions left out by the average performance approach and to capture resilience levels when multiple disruptions occur. The importance of PIs and NPIs in a dynamic scenario reassembles real settings and enables the potential improvement of the absorptive and restorative capacities simultaneously. Finally, there is a need to assess resilience for communities with different demographic distribution and alternative viruses.

References

[1] Center for disease control and prevention, "Es-

timated influenza illnesses, medical visits, hospitalizations, and deaths averted by vaccination in the united states," 2016. [Online; accessed 11-April-2017].

[2] World Health Organization, "Summary and assessment, 14 february to 16 march 2017," 2017. [Online; accessed 31-March-2017].

[3] World Health Organization, "Analysis of recent scientific information on avian influenza a(h7n9) virus," 2017. [Online; accessed 11-April-2017].

[4] N. M. Ferguson, D. A. Cummings, S. Cauchemez, C. Fraser, S. Riley, M. Aronrag, and et al., "Strategies for containing an emerging influenza pandemic in southeast asia," *Nature*, vol. 437, no. 7056, pp. 209–214, 2005.

[5] N. M. Ferguson, D. A. Cummings, C. Fraser, J. C. Cajka, P. C. Cooley, and D. S. Burke, "Strategies for mitigating an influenza pandemic," *Nature*, vol. 442, no. 7101, pp. 448–452, 2006.

[6] World Health Organization, "Cumulative number of confirmed human cases for avian influenza a(h5n1) reported to who, 2003-2016," 2016. [Online; accessed 30-March-2017].

[7] S. S. Shrestha, D. L. Swerdlow, R. H. Borse, V. S. Prabhu, L. Finelli, C. Y. Atkins, and et al., "Estimating the burden of 2009 pandemic influenza a (h1n1) in the united states (april 2009–april 2010)," *Clinical Infectious Diseases*, vol. 52, no. suppl 1, pp. S75–S82, 2011.

[8] J. R. Santos, K. D. S. Yu, S. A. T. Pagsuyoin, and R. R. Tan, "Time-varying disaster recovery model for interdependent economic systems using hybrid input–output and event tree analysis," *Economic Systems Research*, vol. 26, no. 1, pp. 60–80, 2014.

[9] M. J. Orsi and J. R. Santos, "Estimating workforce-related economic impact of a pandemic on the commonwealth of virginia," *IEEE Transactions on Systems, Man, and Cybernetics-Part A: Systems and Humans*, vol. 40, no. 2, pp. 301–305, 2010.

[10] A. Plough, J. E. Fielding, A. Chandra, M. Williams, D. Eisenman, K. B. Wells, G. Y. Law, S. Fogleman, and A. Magaña, "Building community disaster resilience: perspectives from a large urban county department of public health," *American Journal of Public Health*, vol. 103, no. 7, pp. 1190–1197, 2013.

[11] Center for disease control and prevention, "Principles of epidemiology in public health practice, third edition. an introduction to applied epidemiology and biostatistics," 2012. [Online; accessed 21-April-2017].

[12] S. Riley, J. T. Wu, and G. M. Leung, "Optimizing the dose of pre-pandemic influenza vaccines to reduce the infection attack rate," *PLoS Med*, vol. 4, no. 6, p. e218, 2007.

[13] B. Maguire, P. Hagan, *et al.*, "Disasters and communities: understanding social resilience," *Australian Journal of Emergency Management, The*, vol. 22, no. 2, p. 16, 2007.

[14] M. Keck and P. Sakdapolrak, "What is social resilience? lessons learned and ways forward," *Erdkunde*, pp. 5–19, 2013.

[15] C. Folke, S. R. Carpenter, B. Walker, M. Scheffer, T. Chapin, and J. Rockstrom, "Resilience thinking: integrating resilience, adaptability and transformability," 2010.

[16] C. S. Holling, "Resilience and stability of ecological systems," *Annual review of ecology and systematics*, vol. 4, no. 1, pp. 1–23, 1973.

[17] B. D. Youn, C. Hu, and P. Wang, "Resilience-driven system design of complex engineered systems," *Journal of Mechanical Design*, vol. 133, no. 10, p. 101011, 2011.

[18] G. E. Richardson, "The metatheory of resilience and resiliency," *Journal of clinical psychology*, vol. 58, no. 3, pp. 307–321, 2002.

[19] A. Rose, "Defining and measuring economic resilience to disasters," *Disaster Prevention and Management: An International Journal*, vol. 13, no. 4, pp. 307–314, 2004.

[20] S. Carpenter, B. Walker, J. M. Anderies, and N. Abel, "From metaphor to measurement: resilience of what to what?," *Ecosystems*, vol. 4, no. 8, pp. 765–781, 2001.

[21] S. Y. Ponomarov and M. C. Holcomb, "Understanding the concept of supply chain resilience," *The International Journal of Logistics Management*, vol. 20, no. 1, pp. 124–143, 2009.

[22] S. Hosseini, K. Barker, and J. E. Ramirez-Marquez, "A review of definitions and measures of system resilience," *Reliability Engineering & System Safety*, vol. 145, pp. 47–61, 2016.

[23] S. L. Cutter, L. Barnes, M. Berry, C. Burton, E. Evans, E. Tate, and J. Webb, "A place-based model for understanding community resilience to natural disasters," *Global environmental change*, vol. 18, no. 4, pp. 598–606, 2008.

[24] R. Francis and B. Bekera, "A metric and frameworks for resilience analysis of engineered and infrastructure systems," *Reliability Engineering & System Safety*, vol. 121, pp. 90–103, 2014.

[25] A. Asadzadeh, T. Kötter, and E. Zebardast, "An augmented approach for measurement of disaster resilience using connective factor analysis and analytic network process (fanp) model," *International Journal of Disaster Risk Reduction*, vol. 14, pp. 504–518, 2015.

[26] S. L. Cutter, "The landscape of disaster resilience indicators in the usa," *Natural Hazards*, vol. 80, no. 2, pp. 741–758, 2016.

[27] M. Bruneau, S. E. Chang, R. T. Eguchi, G. C. Lee, T. D. O'Rourke, A. M. Reinhorn, M. Shinozuka, K. Tierney, W. A. Wallace, and D. von Winterfeldt, "A framework to quantitatively assess and enhance the seismic resilience of communities," *Earthquake spectra*, vol. 19, no. 4, pp. 733–752, 2003.

[28] C. W. Zobel, "Representing perceived tradeoffs in defining disaster resilience," *Decision Support Systems*, vol. 50, no. 2, pp. 394–403, 2011.

[29] G. P. Cimellaro, O. Villa, and M. Bruneau, "Resilience-based design of natural gas distribution networks," *Journal of Infrastructure Systems*, vol. 21, no. 1, p. 05014005, 2014.

[30] C. W. Zobel and L. Khansa, "Characterizing multi-event disaster resilience," *Computers & Operations Research*, vol. 42, pp. 83–94, 2014.

[31] B. M. Ayyub, "Practical resilience metrics for planning, design, and decision making," *ASCE-ASME Journal of Risk and Uncertainty in Engineering Systems, Part A: Civil Engineering*, vol. 1, no. 3, p. 04015008, 2015.

[32] M. Ouyang and L. Dueñas-Osorio, "Time-dependent resilience assessment and improvement of urban infrastructure systems," *Chaos: An Interdisciplinary Journal of Nonlinear Science*, vol. 22, no. 3, p. 033122, 2012.

[33] P. H. Longstaff and S.-U. Yang, "Communication management and trust: their role in building resilience to surprises such as natural disasters, pandemic flu, and terrorism," *Ecology and Society*, vol. 13, no. 1, p. 3, 2008.

[34] T. K. Das, A. A. Savachkin, and Y. Zhu, "A large-scale simulation model of pandemic influenza outbreaks for development of dynamic mitigation strategies," *Iie Transactions*, vol. 40, no. 9, pp. 893–905, 2008.

[35] A. Uribe-Sánchez, A. Savachkin, A. Santana, D. Prieto-Santa, and T. K. Das, "A predictive decision-aid methodology for dynamic mitigation of influenza pandemics," *OR spectrum*, vol. 33, no. 3, pp. 751–786, 2011.

[36] D. L. Martinez and T. K. Das, "Design of non-pharmaceutical intervention strategies for pandemic influenza outbreaks," *BMC public health*, vol. 14, no. 1, p. 1, 2014.

[37] D. L. Martinez Torres, "Non-pharmaceutical intervention strategies for pandemic influenza outbreaks.," 2013.

[38] M. A. Miller, C. Viboud, M. Balinska, and L. Simonsen, "The signature features of influenza pandemicsimplications for policy," *New England Journal of Medicine*, vol. 360, no. 25, pp. 2595–2598, 2009.

[39] C. W. Zobel and L. Khansa, "Quantifying cyberinfrastructure resilience against multi-event attacks," *Decision Sciences*, vol. 43, no. 4, pp. 687–710, 2012.

About the Author

Walter Silva-Sotillo received his B.S. in Industrial Engineering from Pontificia Universidad Católica del Perú in Lima, Peru. In 2005, he received his M.S in Applied Mathematics for making Decision from Université d'Orléans, France and his M.Eng. in Industrial Engineering from University of South Florida in 2014. He received his Ph.D. in Industrial and Management Systems Engineering from the University of South Florida in 2017. His areas of research include simulation of pandemic influenza outbreaks, data analytics, and resilience methods.